308 --- Q200312080004

Scientific Notebooks No. 050: Investigation on Microstructural Analysis and Phase Identification of Uranium-Containing Samples (06/15/1992 through 12/19/1996)

21
300

R

Yi-Ming Pan

Contents

Entries on pages 1 to 63 were made by Yi-Ming Pan.

ECP
7/21/94

Contents

Investigation of Natural Uraninite Alternation of Nopal I

(Initial Entry) 6/15/92

This notebook documents the investigation on microstructural analysis and phase identification of uranium-containing samples using the SwRI Philips 301 scanning transmission electron microscope (STEM).

The STEM provides the capabilities for high magnification analysis up to 500,000X, and diffraction and microdiffraction for crystallography/structure analysis. These information can be aid in the interpretation of observations with petrographic microscopy and scanning electron microscopy (SEM) and provide an understanding of the mineral alteration.

6/15/92 RCE

TEM Foil Sample Preparation (Granular Uraninite)
Batch-1 6/16/92

Summary of previous work on TEM sample preparation and analysis of uranium-containing samples provided by Dr. English Pearcy (10/8/91).

TEM thin foil preparation:

- The sample preparation started from thin sections of thickness around 30 μm for petrographic analysis.
- Disks 3mm in diameter were punched out from the areas of interest, including black area, yellow area, and yellow veinlet.
- The disks were then placed in the Gatan ion-beam milling machine for further thinning to obtain the desired electron transparent region near the perforated area. The operating conditions for ion milling were:

  3.5 kV Gun Voltage
  1 mA Gun Current (2 Guns / 0.5 mA each)
  12-22.5° Tilt Angle
  Liquid Nitrogen in Cold Trap

- Samples were coated with carbon at 6 KV, 1 mA, 30° tilt for 4 min.

Note: In many cases, disks were mounted on copper supporting ring with epoxy because of the problem of disk breakage during handling.

ECP 8/25/94

Summary of TEM foils prepared at SwRI

Sample I.D.	Area of Interest	Milling time (total hours)	Remark
U1-1	black/yellow interface	9.6 hrs	Both samples were broken during handling w/o supporting ring
U2-1	"	11.6 hrs	
U2-2	black area	17.3 hrs	
U2-3	yellow area	13 hrs	
U2-4	black area	31.8 hrs	

Note: While thin section U1 was a sample away from the uranium source of the hydrothermal deposit, thin section U2 was a sample close to the deposit.

ECP 8/25/94

TEM Observation of Granular Uranmite 6/17/92

TEM Analysis

The thin foil specimens were examined in the TEM operated at 100 kV.

1) U2-2

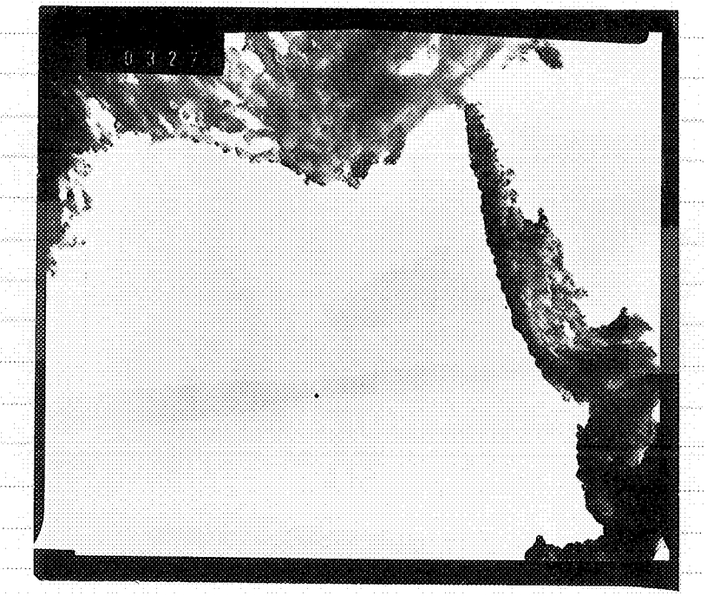

Negative No. 3278 8,800 X

2) U2-3

No. 3280
7,500X

No. 3281
18,000X

8/25/94

3) U2-9

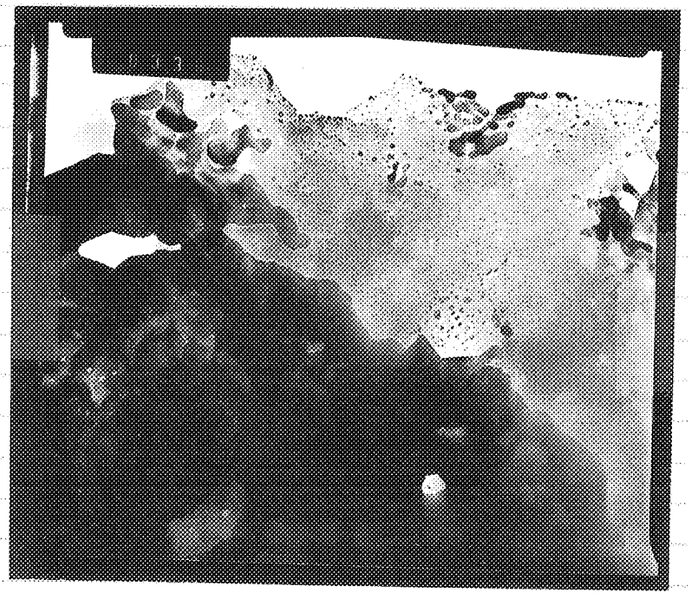

No. 3300
75,000X

* Arrays of artefactual island structures due to ion-beam thinning.

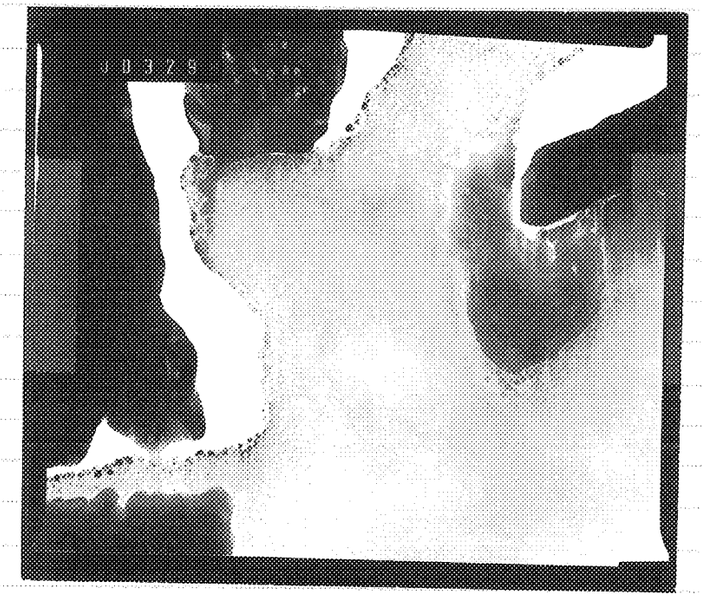

No 3298
75,000 X

Summary of TEM observation on the foils prepared at SwRI.

- TEM observation indicated that the perforated area is very porous (Negative No. 3278) and the electron transparent region around the perforated area is very limited (Negative No. 3280). This may be due to 1) the porous nature of the material or 2) differential thinning of the inhomogeneous material.

- As seen in Negative No. 3300 and 3298 of U2-9, arrays of artefactual island structures are found at the edges of the perforated area. These artefacts are believed due to specimen heating during ion-beam thinning. Previous studies have shown that energy input the specimen by ion-beam thinning process is sufficient to raise the specimen temperature up to 370°C, and to cause microstructural instability. It is perhaps reasonable to speculate that dehydration may be occurred in the current rock sample which contains kaolinite and uranyl hydrates.

Suggestion: The heating effect, however, can be eliminated by the use of a low-temperature, cooled specimen support, so called Liquid Nitrogen Cold Stage, during ion beam thinning.

ECA 8/25/94

Granular Uraninite TEM Samples Preparation at Rice University (Batch - 2)

6/29/93

TEM sample preparation at Rice University

Contact: Dr. Daniel L. Callahan
Assistant Professor
Department of Mechanical Eng. and Materials Science
Rice University
(713) 527-8101 Ext. 3572

- Seven disk samples were punched out from thin sections: U1 & U2 and sent to Dr. Callahan as follows.

Yellow Area	DY1, DY2	] from U1
Black Area	DB3, DB4, DB5	
Yellow Violet	AV6, AV7 (from U2)	

- Four TEM foils, DY1, DB3, DB5 & AV6, were prepared and mailed to us. The disks from thin sections were further mechanically thinned to form a dimple approximately 10 μm thick, and were then mounted on supporting rings. The TEM foils were perforated using a Gatan ion mill with a liquid nitrogen cold stage under the conditions like we did.

EH 6/25/94

Thin foils inspected with optical microscope:

TEM foils inspection showed that samples from black area (DB3 & DB5) exhibit differential milling, resulting in porous perforated areas, while sample AV6 from yellow-violet shows a dense perforated area. For sample DY1, a large perforated area is observed with very limited thin region.

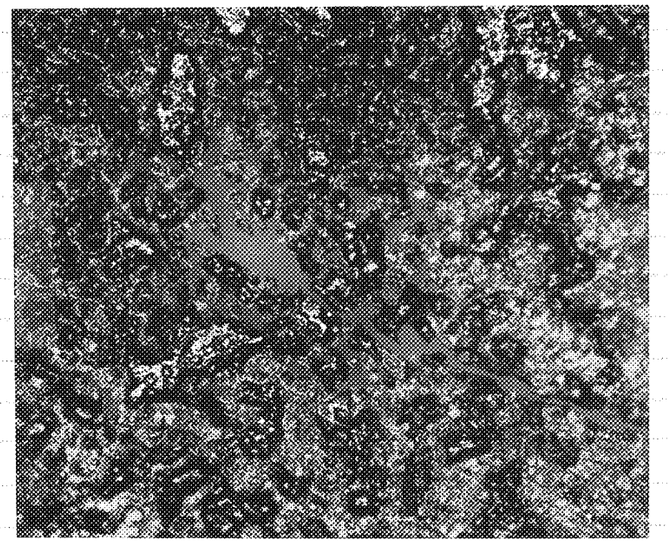

Optical photograph
DB3
No. 0558-1
201.6 X

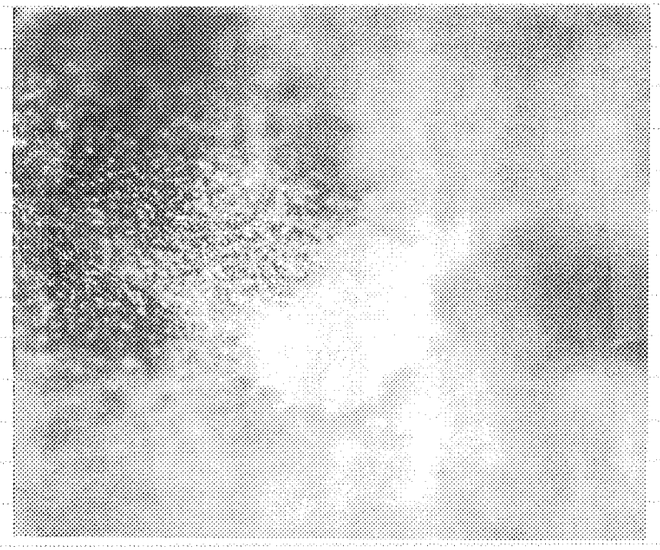

DB5
No. —
201.6 X

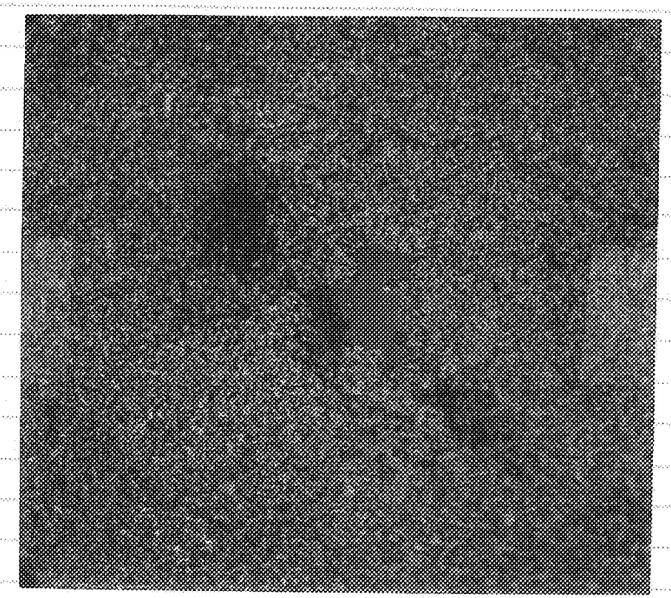

AV6
No. 055852
201.6X

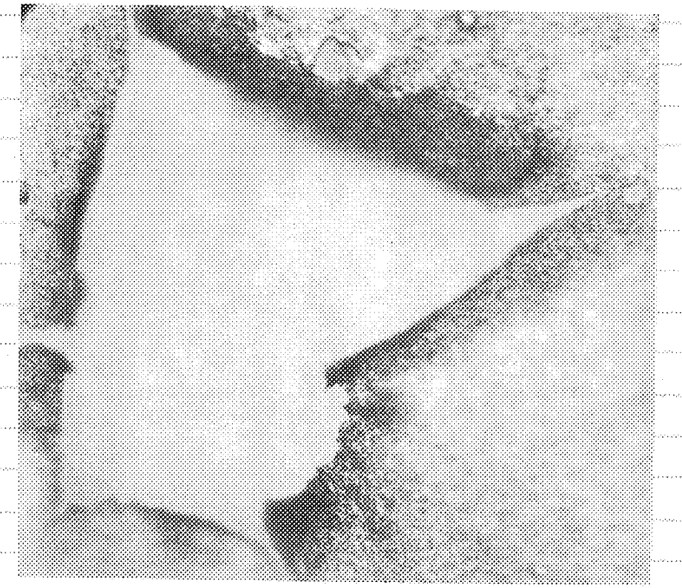

DY1
No. —
201.6X

TEM Analysis

Preliminary TEM observation of the samples prepared at Rice University was done and TEM photographs were taken at different magnifications.

1) DB 3

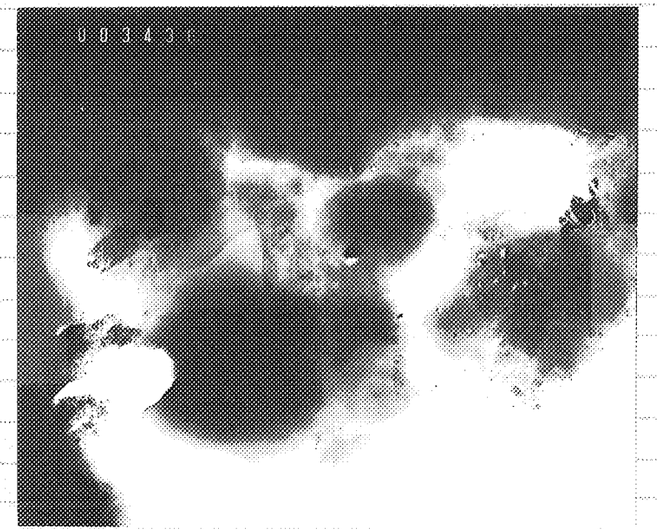

No. 3436
4,300X

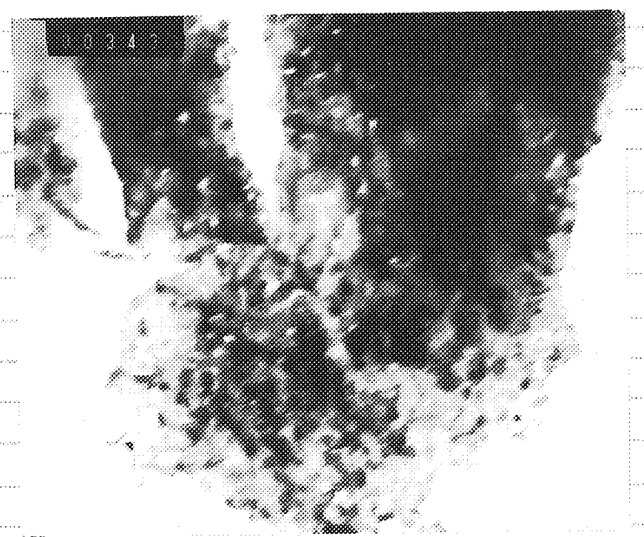

No. 3437
59,000X

2) DB5

No. 3431
4,300X

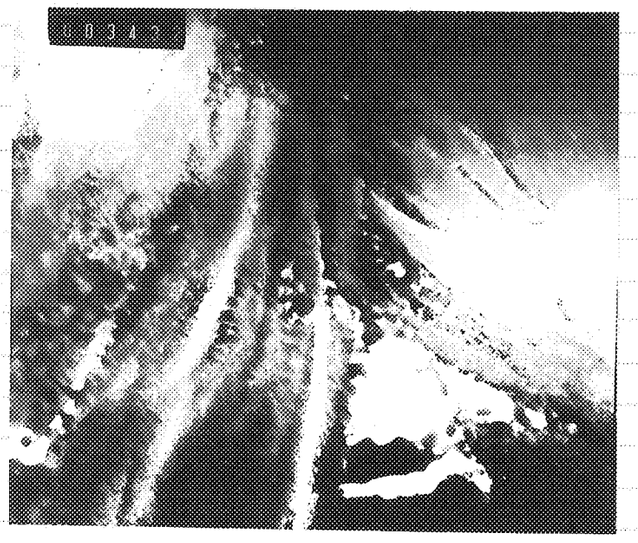

No. 3432
18,000X

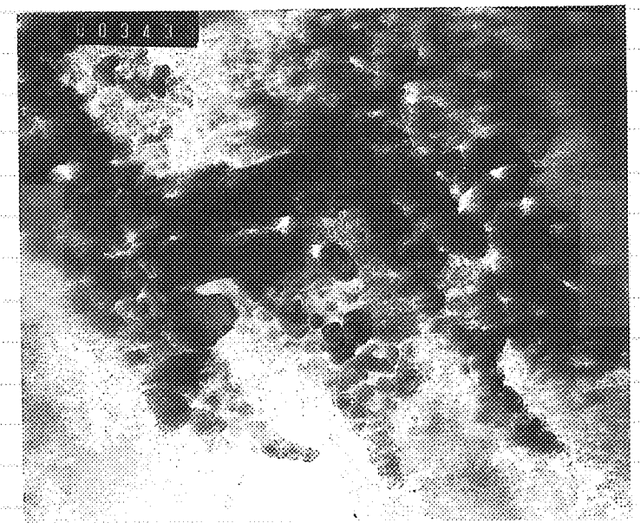

No. 3433
57,000X

3) DY1

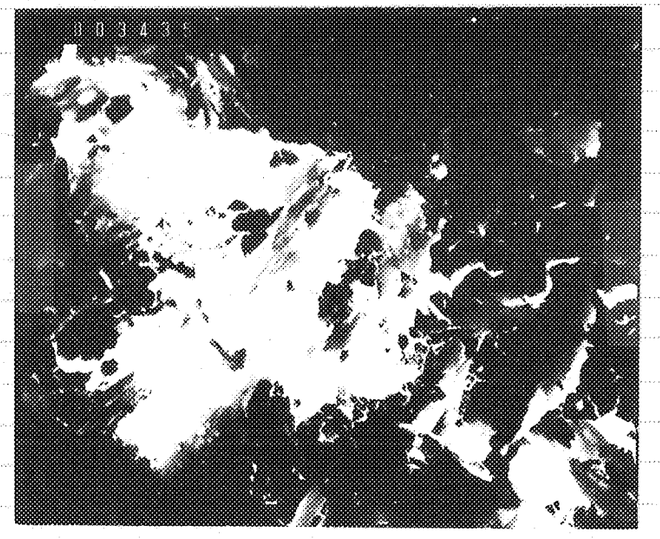

No. 3435
9,300X

4) AV6

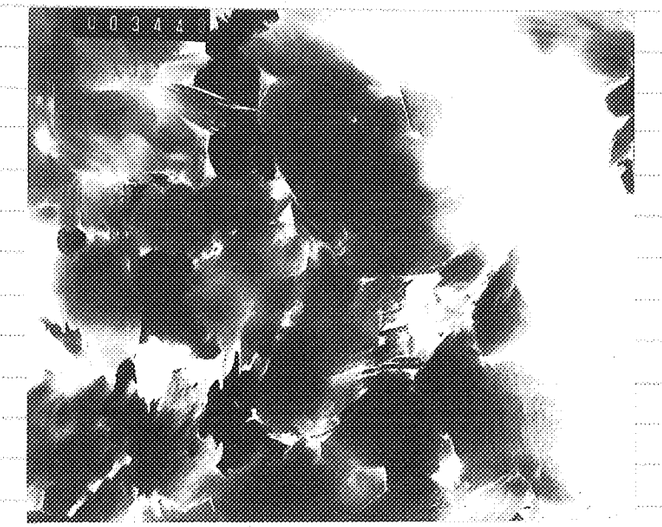

No. 3490
4,300X

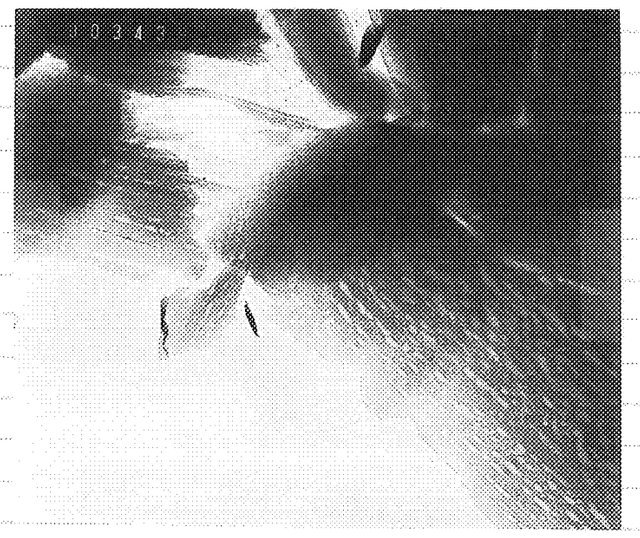

No. 3439
32,000X

SEM/EDS Analysis of Batch 2 Granular Uranyite
TEM Samples
9/27/92

SEM Analysis

- In an attempt to correlate the TEM observation with that of SEM, the TEM foils were glued on to a graphite plate with colloidal graphite and then examined under the SEM.

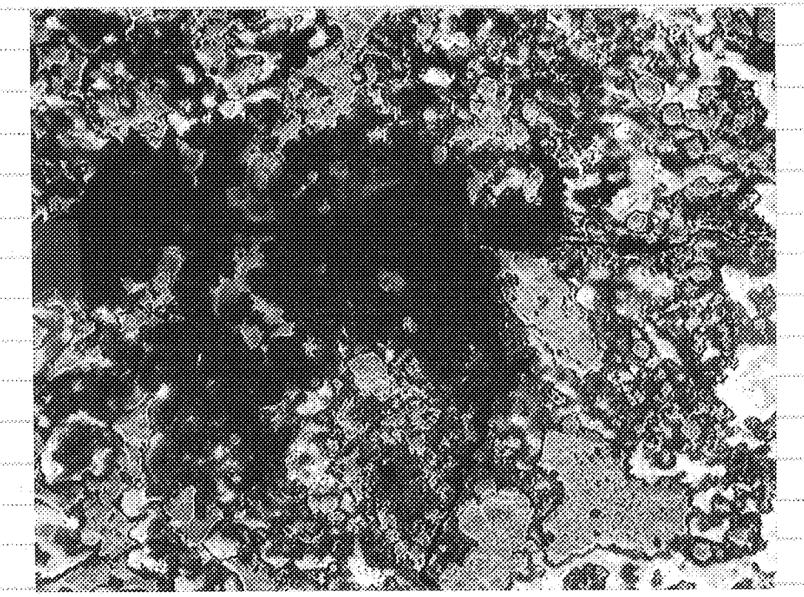

DB3
No. 56156
300X

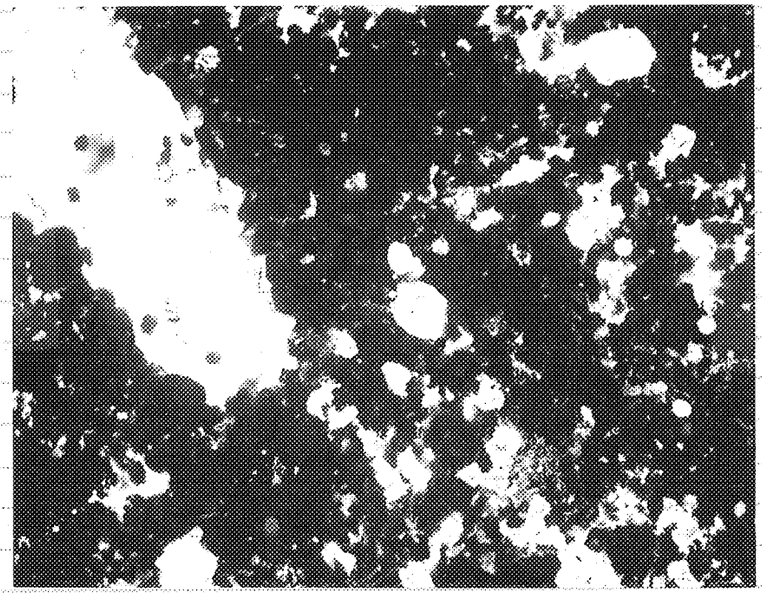

No. 56158
1,000X
BSE Image

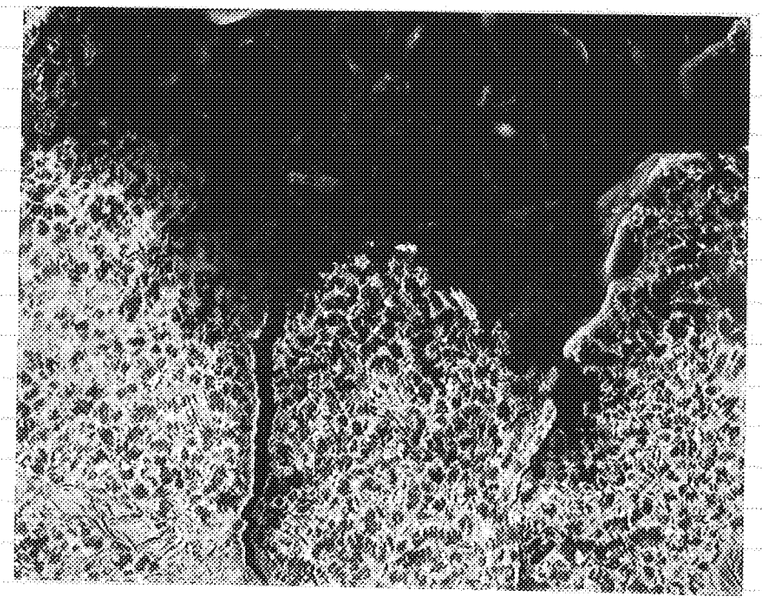

DB5

No. 56161

500X

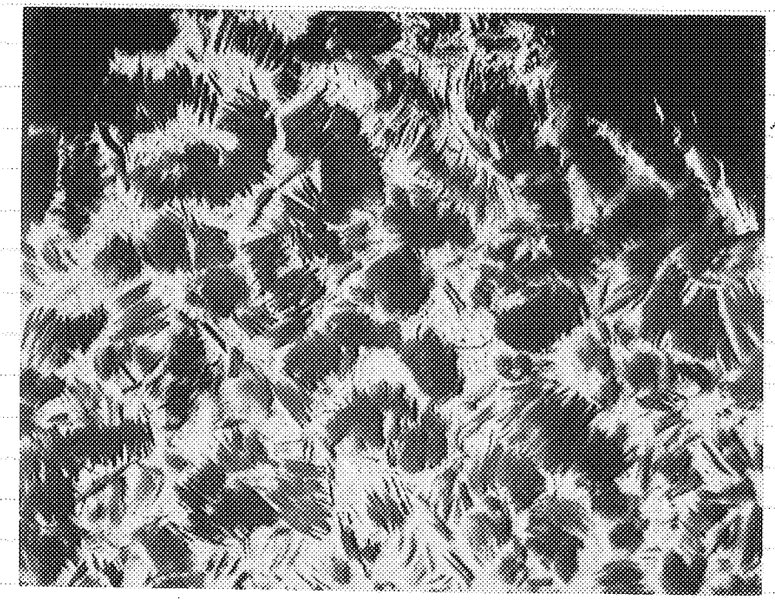

No. 56165

3,000X

BSE Image

EDX Results (Energy Dispersive x-Ray Analysis)

Foil I.D.	Location (BSE Image)	Major Element	Possible Mineral
DB 3	Black	Si	Quartz
	white	U	Uraninite
DB 5	Black	Al, Si	Kaolinite
	white	U	Uraninite
AV6	Black	Al, Si	Kaolinite
	white	U, Al, Si	Soddyite (?)

Note: Effect of Al-stud has been blocked out by the use of a graphite plate.

* Status of TEM foils removed from SEM sample studs:

DB 3	O.K.
DB 5	Chipping at the perforated area
AV6	O.K.
DY 1	Lost.

ECP 8/25/84

TEM Diffraction Analysis of Batch 2 - DB5 Sample

7/29/92

TEM Diffraction Analysis of foil DB5

Selected area diffraction patterns (SADP) were taken from different locations of the DB5 TEM image (No 3459). The camera constant was # 1192 ($\lambda L = 48.5744$ mm·Å).

$\lambda L = Dd$
↑ transfer

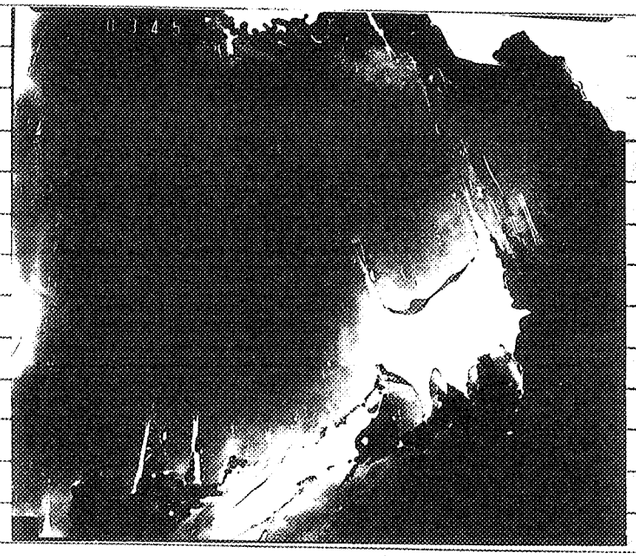

No. 3459
22,000X

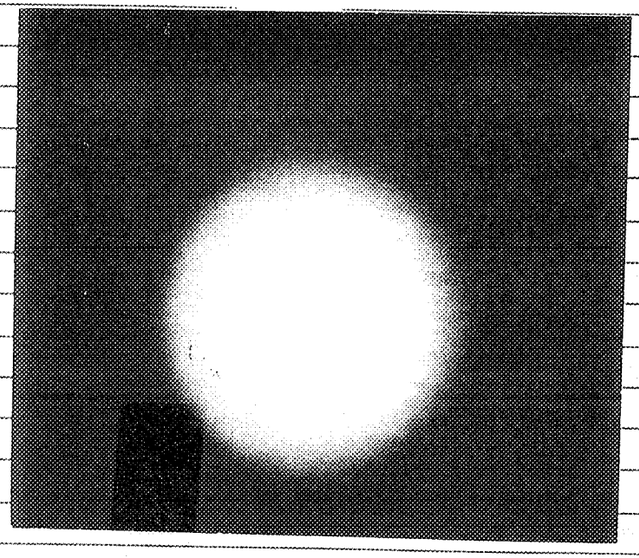

No. 3458
From center of No. 3459

* The diffuse ring pattern indicates an amorphous phase.

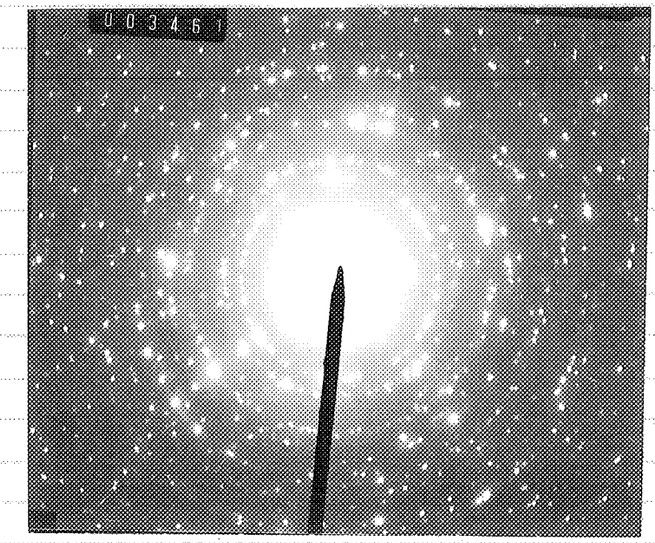

No. 3461
From the fine grain area of the lower left-edge of No. 3459

* the spot/ring pattern indicate fine-grain polycrystalline phases.

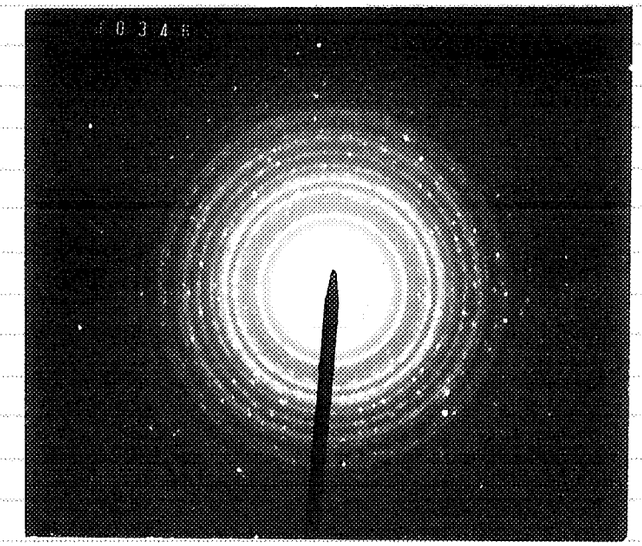

No. 3464
From No 3459

* this DP may be a mixture of amorphous and polycrystalline.

7/30/92

Indexing of DP No. 3461

1. Procedure for indexing spot/ring patterns will be treated as ring patterns as follows.

   a) Measure the ring diameters (2R).
   b) Determine the ratios of the squares of the diameters of the outer rings to that of the first ring.
   c) Check the ratios against the ratios of the possible reflections of the crystal structure of interest.

$d = \frac{\lambda L}{2R}$ $\qquad D^2 = \frac{h^2+k^2+l^2}{(L\lambda)^2}$

Ring No.	Diameter (2R)	d(Å)	$(2R)^2$	Plane	d(Å)	$(2R)^2/(2R_1)^2$	$R^2 \cdot \frac{a^2}{(L\lambda)^2}$	
1	19.0	3.08	361	(111)	3.16	1	0.99	3.16
2	22.0	2.66	484	(200)	2.74	1.34	1.06	4.24
3	30.4	1.93	924	(220)	1.93	2.56	2.01	8.04
4	35.6	1.64	1267	(113)	1.65	3.51	2.76	11.04
5	43.0	1.36	1849	(400)	1.37	5.12	4.03	16.12
6	47.1	1.24	2218	(331)	1.25	6.14	4.84	19.36

2. In comparison with the crystal structure of uraninite - f.c.c.:

Possible Reflection	$h^2+k^2+l^2$	$(h^2+k^2+l^2)/3$
(111)	3	1
(200)	4	1.33
(220)	8	2.67
(311)	11	3.67
(222)	12	4.00
(400)	16	5.33
(331)	19	6.33

3. From the geometry of the TEM diffraction pattern:

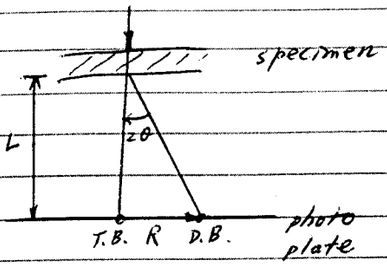

$2d \sin\theta = n\lambda$

If θ is very small,

$2\theta \approx \lambda/d = R/L$

$Rd = L\lambda$

where d: lattice spacing

$L\lambda$: camera constant

For f.c.c structure,

$$\frac{1}{d^2} = \frac{h^2+k^2+l^2}{a^2}$$

$$R^2 \cdot \frac{a^2}{(L\lambda)^2} = h^2+k^2+l^2$$

$$\Rightarrow \boxed{R_1^2/R_2^2 = (h_1^2+k_1^2+l_1^2)/(h_2^2+k_2^2+l_2^2)}$$

- Indexing of DP No. 3461 indicates that the fine grains are phases of f.c.c. structure, probably uraninite. Further distinct spot diffraction patterns need to be taken in identifying phase of UO_2 or U_4O_9.

7/31

- The ratios of R_1^2/R_2^2 are in a good agreement with $(h_1^2+k_1^2+l_1^2)/(h_2^2+k_2^2+l_2^2)$ indicating a f.c.c. structure. However, the products of $R^2 \cdot \frac{a^2}{(L\lambda)^2}$ by using $a(UO_2) = 5.47$ Å and $L\lambda = 58.5744$ mm·Å don't reach the values of $(h^2+k^2+l^2)$ for possible reflections. In fact, there are about 4 times difference.

↖ Dick may use diameter in the calibration of camera const.

D.K.

TEM Analysis Contact at Uni. of New Mexico

8/7/92

- Contact at Uni. of New Mexico for TEM work

Dr. Lumin Wang — Prof. Rodney C. Ewing
Research Associate / TEM microscopist
(505) 277-7536
4458 (TEM)
Dept. of Geology

- Dr. Wang's research interest focuses on radiation-induced crystalline to amorphous transformation and simulated nuclear waste glass reaction with analytical and high resolution electron microscopy.

- TEM facilities at Uni. of New Mexico

HREM Jeol 2000 FX, 200 keV, ~3 Å resolution
STEM TN 5500 EDS, Hot stage ~700°C & Cold stage ~LN temp.
Oxygen analysis can't be done w/o windowless detector in the STEM.

- Experiment Cost

$100/sample for TEM foil preparation
$55/hr for TEM analysis if remains co-laboration.

- Supporting information:

① The presence of amorphous phase in DB5 sample may be due to the uraninite radiation induced amorphization process.

② Concerning the TEM sample preparation, differential milling has been found in the samples consisting of uraninite in a light matrix like clay, low uraninite content in particular. This will result in a porous perforated area. Succesful TEM analysis will rely on luck to find appropriate thin area.

In fact, the TEM analysis at Pacific Northwest Lab.[1] was done on spent fuel which has much higher uraninite content, while the other paper[2] on electon diffraction of U_4O_9 was from single crystal of UO_2.

Ref.:

(1) L. E. Thomas et al., "Microstructural examination of oxidized spent PWR fuel by transmission electron microscopy" J. Nucl. Mater., 166 (1989) 243-251.

(2) H. Blank and C. Ronchi, "Electron diffraction of U_4O_9" Acta Cryst. A24 (1968) 657-666.

8/25/94

Granular Uraninite TEM Samples - Batch 3

9/28/92

TEM samples preparation @ Univ. of New Mexico

- The objective of this work is to analyze different states of oxidation of the uraninites as a result of mineral alteration.
- Three 3mm disk samples have been punched out from a thin section, NOPI-ECPI-T52, for TEM thin foil preparation, as marked on the photograph below. While U1 is from the isolated black area, U2 & U3 are close to the yellow area.
- As can be seen in Photo 5, taken from sample U1 with a field-of-view of 0.5 mm, the uraninites in white color have intergrown with other minerals, including kaolinite in dark gray, and uranium silicates in various shades of gray.

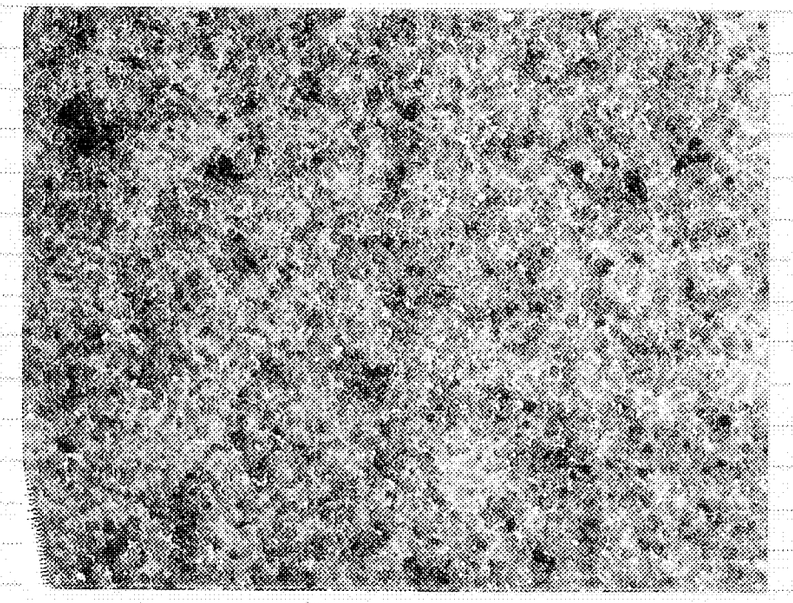

Photo 5 of U1
FOV: 0.5 mm

White: uraninite
Dark gray: kaolinite
Various shades of gray: uranium silicates

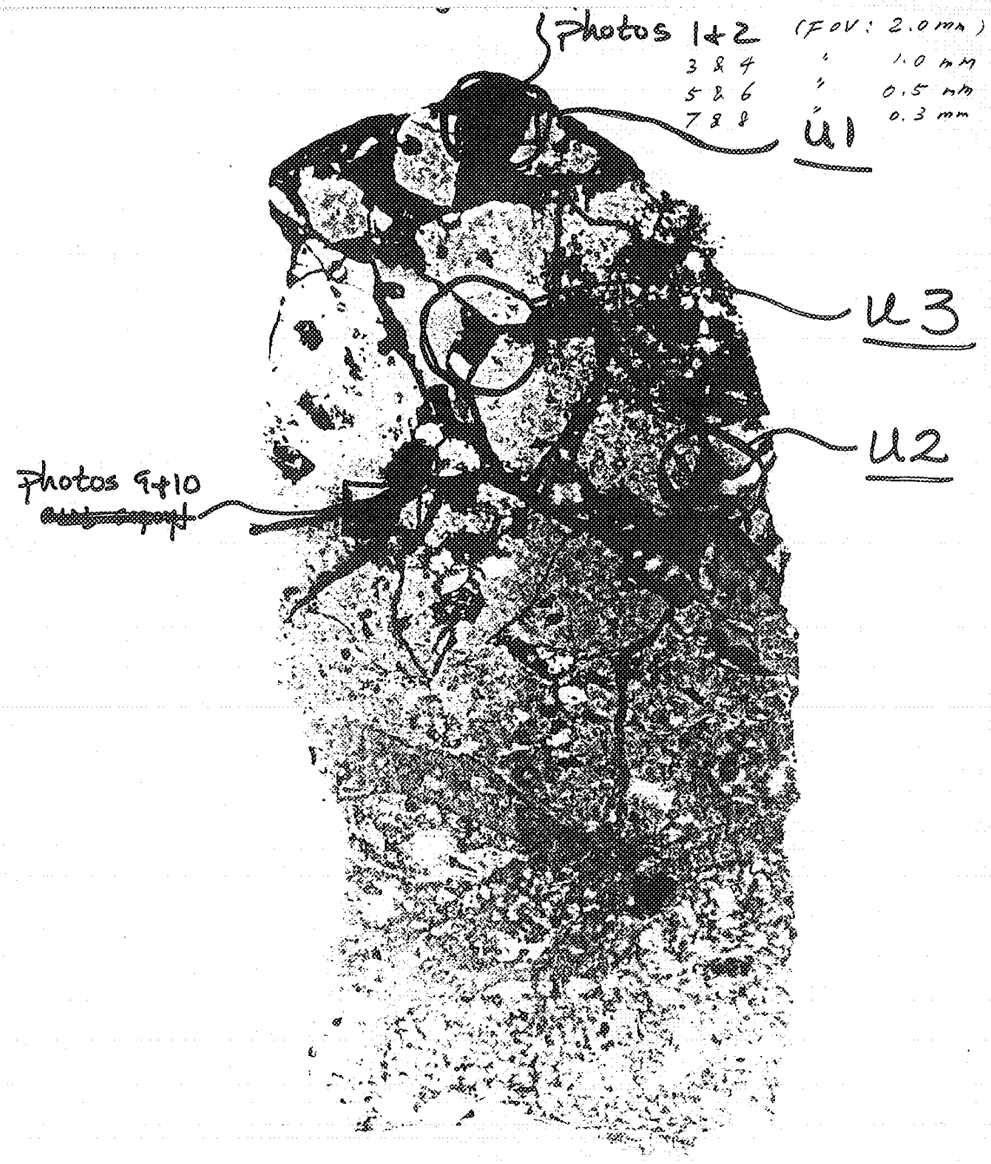

Crystal Structure of Major Minerals

10/6/92

ASTM Powder Diffraction Files

Mineral	D Spacing (I/I,)	Lattice Constant	File No.
Uraninite			
UO_2	3.15(100), 2.73(50), 1.93(50), 1.65(45)	Cubic (F, C, C) $a=5.4682$	41-1422 ~~5-0550~~
U_4O_9	1.64(100), 3.12(90), 1.92(90), 2.72(60)	Cubic $a=5.440$	9-206
Kaolinite	7.15(100), 3.57(100), 2.33(90)	Triclinic $a=5.14$, $b=8.93$, $c=7.37$	5-0143
$Al_2Si_2O_5(OH)_4$			
Quartz (α)	3.34(100), 4.26(35), 1.82(17)	Hexagonal $a=4.913$, $c=5.405$	5-0490
SiO_2			
Soddyite	4.57(100), 6.28(90), 3.36(90)	Orthorhombic $a=8.32$, $b=11.21$, $c=18.71$	8-195 12-180
$(UO_2)_2(SiO_4)_2(OH)_2\cdot 5H_2O$	3.32(100), 4.48(90), 6.14(80)		
Weeksite	7.11(100), 5.57(90), 8.88(80)	Orthorhombic $a=14.26$, $b=35.88$, $c=14.20$	12-462
$K_2(UO_2)_2(Si_2O_5)_3\cdot 4H_2O$			
Uranophane	7.88(100), 3.94(90), 2.99(80)	Monoclinic $a=15.87$, $b=7.05$, $c=6.66$, $\beta=97°15'$	8-442
$CaO\cdot 2UO_3\cdot 2SiO_2\cdot 6H_2O$			

EC 8/25/94

2/12/93

TEM Experment at UNM

Obj.: Identify states of oxidation of the uraninites, white color under reflected light, as an index of mineral alternation and in support of the previous microprobe analysis.

Exp.: TEM analysis was performed on thin foils U1 and U2 under JOEL 2000 STEM.

	Neg. No.	DP or Mag. 100 K	Note	EDS (200 Å)
U1	9,946 439106	DP	DP of Kaolinite	
	9107	DP		
	9108	8.5K	intergrown area	
	9109	34 K	"	
	9110	34 K	"	
	9111	DP	dark region	U1-1 (U, Cu) ← Copper grid
Kaolinite?	9112	DP	white region	U1-2 (Al, Si)
	9113	DP	DP of a strip	
	9114	100 K	strip morphology	
	9115	170 K	"	U1-3 (U, Cu)
	9116	DP	DP at the tip of a strip	"
	9117	DP	"	
	9118	17 K	strip morphology	
	9119	50 K	"	
	9120	50 K	"	
	9121	170 K	"	
	9122	DP	Dark regin of UO_2	
U2	9123	DP	Dark regim of smaller particles (ring pattern)	

EC 8/30/94

Remark: 1) All the diffraction patterns were taken with an aperture of ~2.5μm (3cm at 68K) and a camera constant of $\lambda L = 2.35$ cm·Å.

2) the aperature size for EDS is about 200Å.

Neg. No	DP/Mag.	Note	EDS
U2			
939124	170K	granular morphology ①	U, Cu, Pb (Not Saved)
X 9125		" ②	"
9126	DP		
9127	100K	strip morphology	
9128	130K	granular morphology ②	
9129	DP	DP of polycrystal w/ preferred orientation	
9130	DP		
9131	170K	granular morphology	
9132	170K	"	
9133	DP		
9134	DP	DP of a large particle	U, Cu, Pb, Si
9135	68K	a large particle	
9136	34K	intergrown structure	
9137	DP	(dark) White strip in 9136	U, Cu, Si
9138	DP	White region in 9136	Al, Si
9139	34K	black islands	
9140	DP	black region	U, Cu, Pb
9141	DP	White region	Al, Si
X 9142	DP		U, Cu, Si (O)
9143	100K	strip morphology in 9136	At% 50.47 2.76 66.67
9144	DP	DP at the end of the strip	

X No negatives received from UNM.

Q.d 8/25/94

d 9/16/94

Diffraction Pattern Index of Batch 3 Samples

V 63/95

Diffraction Pattern Analysis

- There are four different types of DPs that can be classified as follows:

	Neg. No.	
Type I	9106, 9107, 9138*	spot pattern
II	9111, 9113, 9116, 9117, 9122, 9144	spot pattern
III	9141	
IV	9112+, 9123, 9126, 9129, 9130, 9133, 9134, 9137+, 9140	ring pattern

a.d 6/30/94

* Only one row + extra large d-spacing spots
9112 - possibly from kaolinite (001)
9137 - " (001) & (11T)

- Index of 9106

9106 UO_{2+x} [1$\bar{1}$1]

spot	R(cm)	d(Å)	θ
1	0.55	4.27	412 = 56°
2	0.55	4.27	423 = 88°
3	0.90	2.61	413 = 32°

Calculated results:

spot	plane	d(Å)	θ
1	(1$\bar{1}$0)	3.87	413 = 30°
3	(2$\bar{1}$1)	2.23	

⇒ Zone axis [1$\bar{1}$1]
However, this DP is a complete B.C.C. [1$\bar{1}$1] pattern instead of an F.C.C. [1$\bar{1}$1].
This may be due to the change of the structural factors in in UO_{2+x} structure.
(see p33 [1$\bar{1}$1] DP)

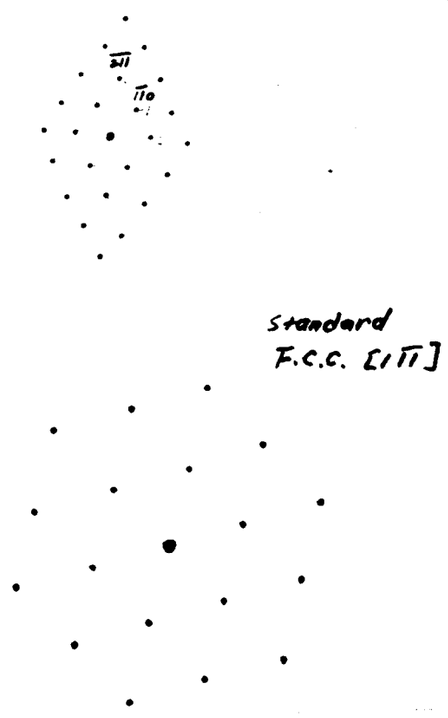

standard F.C.C. [1$\bar{1}$1]

° Index of 9116

Spot	R(cm)	d(Å)	θ
1	0.72	3.24	∠12 = 57°
2	0.85	2.76	∠23 = 91°
3	1.25	1.88	∠13 = 34°

Calculated results:

Spot	plane	d(Å)	θ
1	(11̄1)	3.16	∠12 = 54.7°
2	(002)	2.74	

⇒ Zone axis : [1̄10]

This DP is an exact F.C.C. [1̄10] pattern.

+ Compared to a DP of NOPI-Y powder (3307)

9116

UO_{2+x} [1̄10]

NOPI-Y 3307 (Powder)

UO_{2+x} [1̄10]

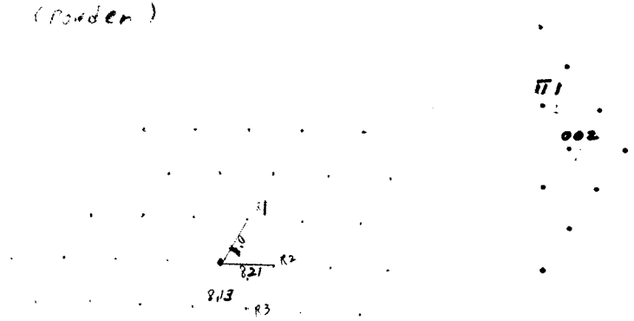

$R_2/R_1 = \frac{8.21}{8.0} = 1.026$

$R_3/R_1 = \frac{8.13}{8.0} = 1.016$

° Index of 9141

	Measured			Calculated		
Spot	R(cm)	d(Å)	θ	Plane	d(Å)	θ
1	0.52	4.52	∠12 = 90°	(11̄0)	3.87	∠12 = 90°
2	1.0	2.35	∠23 = 39°	(1̄12)	2.23	
3	1.09	2.16				

⇒ Zone axis : [1̄11]

However, this DP is not an exact F.C.C. [1̄11] pattern as shown in page 29. Extra spots have been marked as crosses, which may also due to the structural factors.

9141

UO_{2+x} [1̄11]

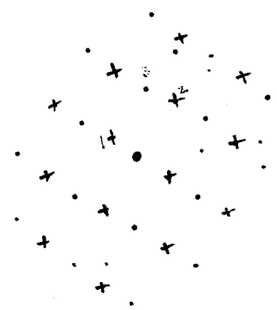

• Index of 9123

Ring No.	Measured D(mm)	Measured d(Å)	Calculated/Possible Reflections $N=h^2+k^2+l^2$	plane	d(Å)	D(mm)
1	14.5	3.24	3	(111)	3.16	14.9
2	16.8	2.80	4	(200)	2.74	17.2
3	23.8	1.97	8	(220)	1.93	24.4
4	28.0	1.68	11	(113)	1.65	28.5
5	29.0	1.62	12	(222)	1.58	29.7
6	33.5	1.40	16	(400)	1.37	34.3
7	36.5	1.29	19	(331)	1.25	37.6
8	41.8	1.12	20 24	(420) (422)	1.22 1.12	38.5 42.0
9	44.0	1.07	27	(333) (511)	1.05	44.8
10	47.8	0.98	32	(440)	0.97	48.4
11	50.5	0.93				

The ring pattern fits very well with the calculated reflections of uraninite.

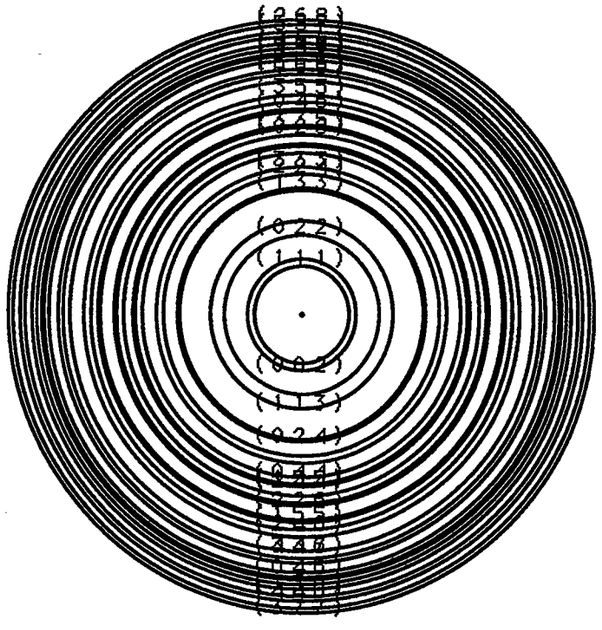

1/27/93

• Calculated UO_2 diffraction pattern with the input of 4 U atoms and 8 O atoms.

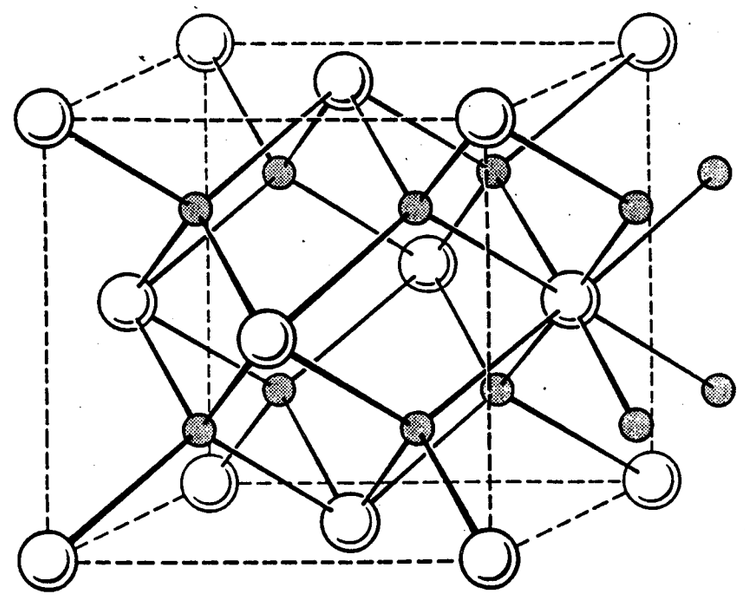

[111]

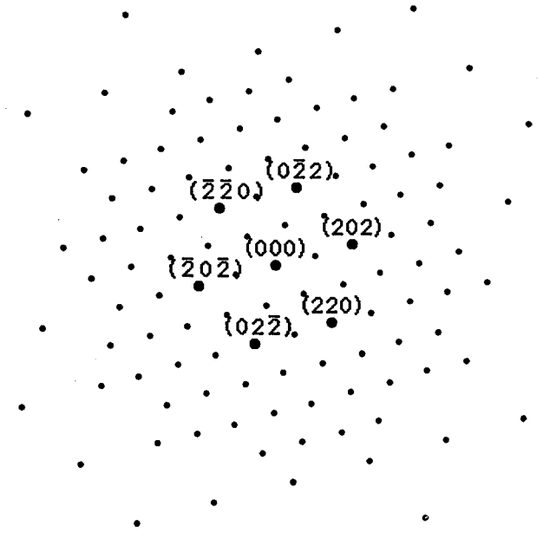

TEM Results Review

2/2/93

Review of the TEM Results with English Pearcy & Jim Pitkay)

- The TEM analyses performed at UNM are generally consistent with the previous TEM and SEM observations, but in greater details and better resolution.

- For the granular structure such as in Photo 9129, 9128, etc, the general morphology of the small grains of sizes 5-100 nm in the granular texture consists of a dark black core surrounded with a layer in gray. EMPA analyses of granular uraninite samples have shown the presence of Ca up to 2 at.%, possibly the uranophane phase. It speculates that the grain morphology is related to uraninite alternation through either the change of the oxygen to uranium ratio or phase conversion. Further analysis is suggested at the lattice image level by high-resolution electron microscopy (HREM).

ECP 8/25/94

HREM Contact

2/5/93

HREM Consideration

- The resolution of direct lattice imaging by HREM is about 5% of the measured lattice spacing. In case of the lattice constant change due to different oxidation state of UO_{2+x}, the lattice spacing varies linearly with composition, $a_o = 5.470 - 0.1080x$ (Å). The value for $x = 0.25$ is 5.443, compared to 5.470 for UO_2. The difference is only 0.5% which is beyond the resolution of HREM.

- Another alternative is to measure the oxygen content across the granular structure using ultra-thin-window EDS technique with HREM. There is no resolution problem to detect different O/U ratios; however, the beam spot size of EDS is the only concern.

- HREM facility contact

  a) HREM Center, Arizona State University
  Roger Graham, User Program Manager (602) 965-7527
  David Smith, Director E-mail: GRAHAM@LA.ASU.EDU

  b) Materials Sci. & Eng. Dept, Northwestern University
  L. D. Marks, Professor (708) 491-7809

ECP 8/25/94

2 of 8 6/30/94

HREM Analysis Proposal to Center for High Resolution Electron Microscopy, Arizona State University

2-18-93

Description of proposed research: (Include a statement of the project aim and its scientific importance and/or technological relevance; preliminary work performed using transmission electron microscopy and other techniques, with appropriate references; details of the proposed microscopy including the techniques you wish to use, the resolution you require, and the microscope(s) you need. Refer to the list of techniques provided or discuss your proposal with Center staff if necessary).

The Center for Nuclear Waste Regulatory Analyses (CNWRA), a federally funded research and development center at Southwest Research Institute (SwRI), is conducting studies of natural systems analogous to important aspects of the proposed high-level nuclear waste repository at Yucca Mountain, Nevada, in support of the US Nuclear Regulatory Commission (NRC). The focus of much of the work is the Nopal I uranium deposit in the Peña Blanca District, Chihuahua, Mexico. The primary ore mineral at Nopal I is uraninite (nominally UO_{2+x}) which is compositionally and structurally similar to spent nuclear fuel (the dominant waste form anticipated for the repository). The hydrology, climate, geochemistry, and geologic structures of the Nopal I deposit are close comparisons to those of the proposed repository site at Yucca Mountain. Uraninite at Nopal I has altered to a suite of secondary minerals including uranyl oxides, uranyl oxyhydroxides, and uranyl silicates. This alteration sequence may represent the long-term corrosion products which may reasonably be expected to form from spent fuel in a Yucca Mountain repository. The processes which govern the initial oxidation of the uraninite and the subsequent formation of uranyl minerals are likely to be important for spent fuel oxidation.

Previous investigations, using optical microscopy, scanning electron microscopy, and scanning transmission electron microscopy, indicate that the uranium mineralization at Nopal I formed as irregularly-shaped masses of fine crystalline uraninite which has been partially altered to uranyl oxyhydroxides and uranyl silicate minerals. Microprobe analyses indicate the uraninite has undergone some degree of oxidation; oxygen to uranium ratios range from 2.03 to 2.48. Microprobe analyses also found significant concentrations of Si (0.22-2.06 at. %) and Al (0.01-1.69 at. %) in all uraninite measurements; many uraninite crystals also have substantial Ca (up to 3.16 at. %). These elements may be incorporated in the uraninite structure or could be present as unrecognized mineral phases that may be intergrown with the uraninite and that are too small to be differentiated by SEM.

Preliminary TEM analyses on thin foils prepared by ion beam thinning techniques were conducted on a Joel 2000 TEM/STEM microscope at the University of New Mexico. The TEM micrographs show crystals of uraninite intergrown with kaolinite; the uraninite and kaolinite identifications were confirmed by EDX microanalysis and electron diffraction analysis. However, the oxidation state of uraninite cannot be differentiated. Some diffraction patterns show extra spots or rings from unrecognized phases with larger lattice parameters, and EDX spectra also indicate the presence of Si, possibly from soddyite (a common uranyl silicate at Peña Blanca) or other as yet unrecognized phases. A common morphology observed was a granular structure of fine uraninite particles on the order of 5-10 nm having a black core surrounded by a diffuse layer in various shades of gray. We speculate that this granular structure may be associated with uraninite alteration through either a change of oxidation state and/or phase transformation.

Unfortunately, the fine uraninite particles were too small for EDX microanalysis and the EDX is also not capable of oxygen analysis. Resolution of these uncertainties requires the application of HREM providing the capability for lattice imaging, microanalysis, and microdiffraction to achieve atomic scale resolution.

In the proposed program, we plan to use HREM to evaluate the mechanisms of uraninite oxidation and to search for potential very small inclusions of Si/Al phases. Specifically, for our initial HREM analyses we plan to define areas of variable oxidation state for the UO_{2+x} series and to search for submicron secondary phases within or adjacent to primary uraninite crystals. This will involve the use of a combination of lattice imaging, EDX microanalysis, and microdiffraction. The VG HB501 microscope, which is capable of EDX analysis for Z>5 with a 1 nm minimum probe diameter, is desirable for qualitative and quantitative elemental analysis including oxygen; the Phillips 400ST-FEG with a 2 nm minimum probe diameter is suitable for lattice imaging and microdiffraction analysis of the fine, granular uraninite structure.

Because the samples to be used are naturally occurring radioactive material, these samples do not fall under any government regulations for radioactive materials. Nevertheless, we handle this material in accordance with established guidelines for regulated radioactive substances. The foils for TEM analysis have contact activities of less than 0.02 mrem/hr. Consequently, the only safety requirements are that ingestion and inhalation be avoided. We anticipate no significant problems meeting these requirements during our HREM analyses.

8/25/94

EC

3/22/93

Approval of the proposal we submitted to ASU:

We have received a letter from Roger Graham, User Program Manager of CHREM that indicated the approval of the proposal. We will contact the staff members to schedule our microscope time during the week of 12th April as follows:

- VG-HB501 [illegible] Mr. Al Higgs (602) 965-3834
- Philips 400ST-FEG Dr. Marija Gajdardziska-Josifovska (602) 965-6177
- JEM-4000EX Dr. Molly McCarthey x4558

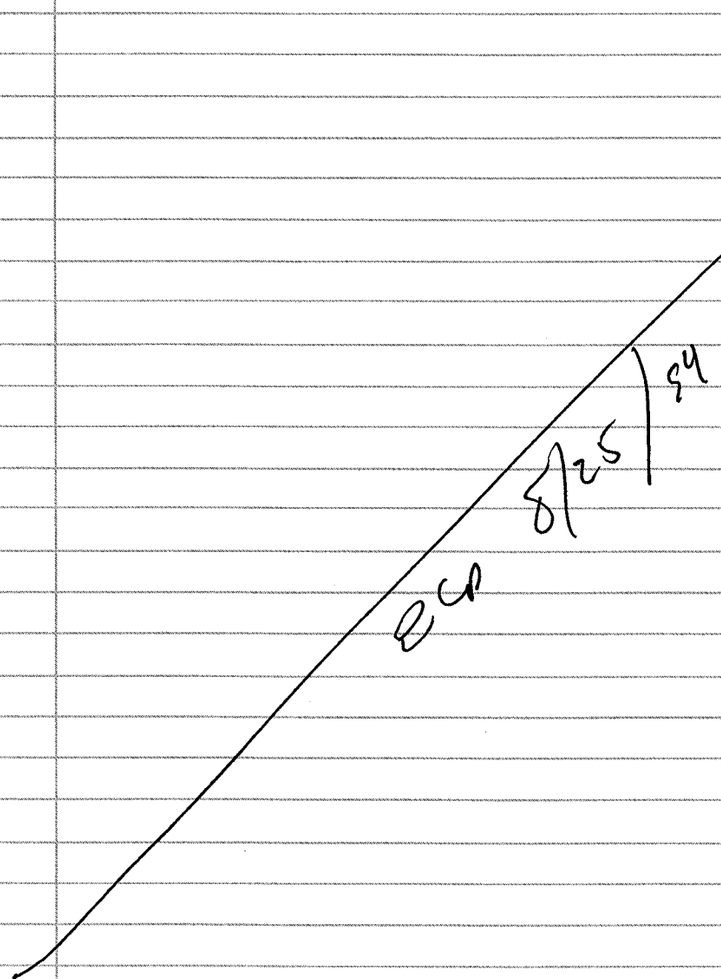

4/28-30/93

HREM Analysis of the Uranophane Samples at ASU

4/28 Philips 400ST-FEG Analysis:

A. Sample U1: Imaging & microdiffraction analysis

Plate No.	Magnification	Remark
Location 1		
405	9,000 x	
406	23,000 x	
407	100 K	
408	340 K	
409	DP	- DP by convergent beam of ~20 Å beam size
410	DP	
411	DP	- CL: 450 mm
412	DP	
413	DP	
414	DP at a zone axis of 410	
415	DP at a zone axis of 413	
416	DP	
417 (2sec)	DP, same as 410	- with a small convergent angle to give a spot pattern
418 (10sec)	DP	
419 (2sec)	DP, same as 416	
420 (10sec)		
421	SADP of the whole area	

Mark locations of each diffraction pattern on plate 407:

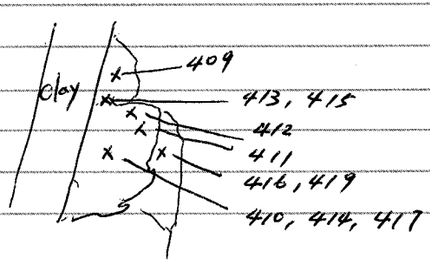

Plate No.	Magnification	Remark
Location 2		
422	9 K	plate 424
423	23 K	
424	100 K	
425	DP	
426	DP	
427	23 K	

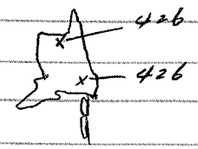

B. Electron Energy Loss Spectroscopy Analysis

EELS Files	Remark
SWRI 01. EEL	Grey area of an isolated particle
02	Dark particle
03	Amorphous
04	Grey area
05	Dark particle
06	Amorphous
07	Thin area of a dark particle
08	Grey area of a dark particle

8/25/94

4/29 Energy Dispersive X-ray Microanalysis with VG-HB501

Sample U1

EDX Files	Remark
Location 1 (see plate 405)	
SWRI 01. xRA	clay
2	Dark particle
3	Large dark particle
4	Grey area
5	Grey area
6	white area
7	Grey area
8	white area
Location 2 (see plate 422)	
SWRI 09. xRA	Dark Particle
10	Grey area
11	white area
12	Grey area
13	Dark particle in the grey area
14	Dark particle
Location 3 (see plate 427)	
SWRI 15. xRA	White area
16	Dark particle

Note: Element mapping was not successful due to beam shifting.

8/25/94

Sample U2

EDX File	Remark
Location 1	
SWR117.XRA	Dark particle
18	Grey area
19	white area
20	Very white area
21	Dark large particle
Location 2	
22	Dark area in a large particle
23	Grey area
24	white area
Location 3	
25	Grey area in a uraninite particle
26	Dark area "
27	White area
Location 4	
28	Dark area in a uraninite particle
29	Grey area "

ECP 8/25/94

4/29 Lattice Imaging with JEM-4000EX

Sample U1 - Location 1

Plate No.	Magnification	Remark
A62303	5,000 (2sec)	intergrown structure
A62304	" (4sec)	} negatives need to be cleaned
A62305	" (5.6sec)	
A62306	" (2.8 sec)	40 obj. aperature
A62307	50 K (2.8 sec)	
A62308	500 K	Lattice image
A62309	↓	
A62310		
A62311		
A62312		
Location 2		
A62313	500 K	
A62314	↓	
A62315		
A62316		
A62317	250 K	
A62318	250 K	
A62319	500 K	
A62320	↓	
A62321		
A62322	50 K	

Sample U3 - Location 1

A62323	500 K
A62324	30 K
A62325	500 K
A62326	↓
A62327	
A62328	

Plate No	Magnification	Remark
Sample U3 - Location 2		
A62329	500 K	
A62330	↓	
A62331	↓	
A62332	↓	
Location 3		
A62333	500 K	
A62334	↓	
A62335	↓	
A62336	↓	
A62337	↓	
A62338	↓	
A62339	250 K	
Sample U 2		
A62340	500 K	
A62341	↓	
A62342	↓	
A62343	200 K	
A62344	500 K	
A62345	↓	
A62346	↓	
A62347	200 K	
A62348	200 K	
A62349	20 K	
A62350	500 K	
A62351	↓	
A62352	↓	Disordered U_4O_9 near edge?
A62353	↓	
A62354	200 K	
A62355	20 K	

Lattice spacing measurements : (calibrated with silicon of 2% accuracy)

Sample U1 #A62308

Region A - 1	grey area	3.148 Å	
2	dark	3.139	) 68.5°
		2.685	
3	grey to white	3.167	
4	white	3.644	
5	white	3.157	

Region B — 6 dark area 2.653 Å
7 " 2.680 } 66.4°
3.004
8 dark to grey 3.142

Region C — 9 dark 3.1095
10 grey to white 3.007
11 white 3.217
12 grey 3.019

Region D grey 1.892

Region E white 3.122

8/25/84

Sample U3 # A 62332

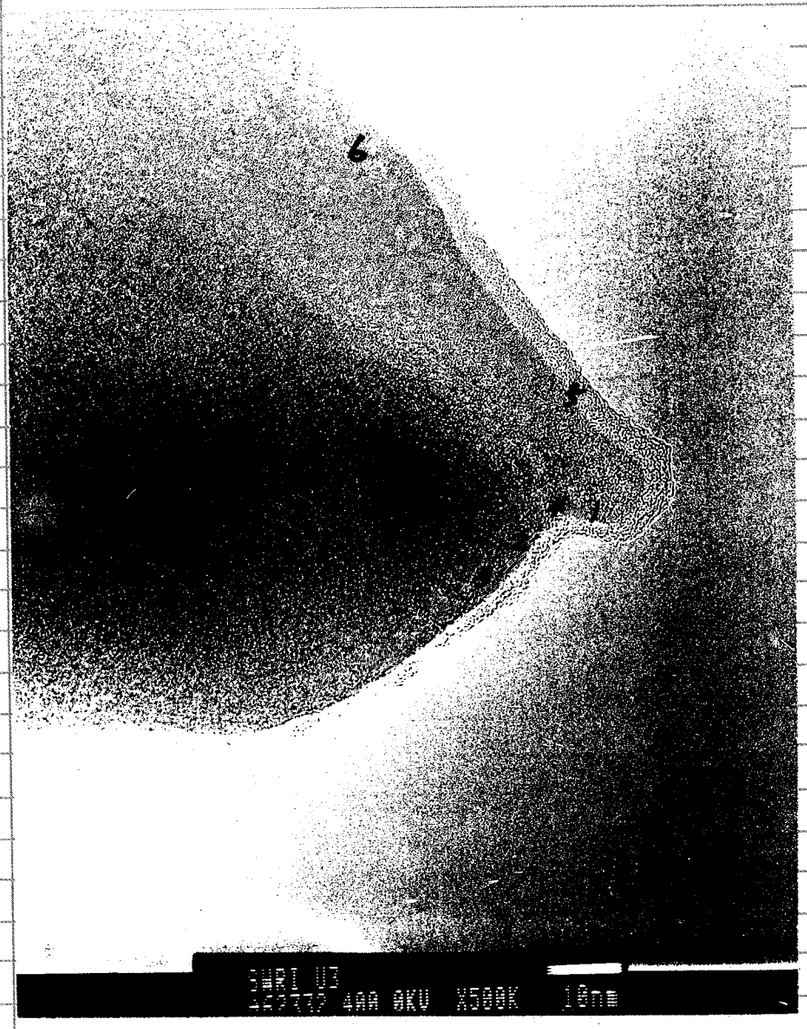

Region 1 3.06 Å } 93.1°
2.64 Å
2 3.12 } 46.6
1.77
3 3.06 } 64.3
3.11
4 3.24 } 58.0
2.98
5 3.107
6 3.045

Sample U3 # A62336

Region 1 amorphous
2 3,023 Å
4.466 Å
} 96.8°
a c
3 ab 3.04
418
} 99.1
x b
qc 2,656
3,043
} 38.6
4 3,014
5 3,099

		Measured		Calibrated
Region 6* – 1	dark area	5,27 Å	88.7	3,138 Å
		5,24 Å		3,120 Å
2	grey	5,246		3,123
		4,621		2.751
3.	white	5,163		3,074
4	white	5,356	28.6	3,189
		3,186		1,897
5.		5,255	90.7	3,129
		3,178		1,892
Region 7	White	4.611	75,3	2,745
		5,188		3,089

* Recalibrated due to change of zoom

Measured	5i spacing	Correction factor	
5,264 Å	3,134 Å	3,134/5,264 = 0,595	0,592
3,265	1,919	1,919/3,265 = 0,588	

8/25/94

Additional HREM Analysis of ASU

7/2/93

Further Lattice Spacing Measurements by Optical Diffractogram

Sample U1 # A 62319

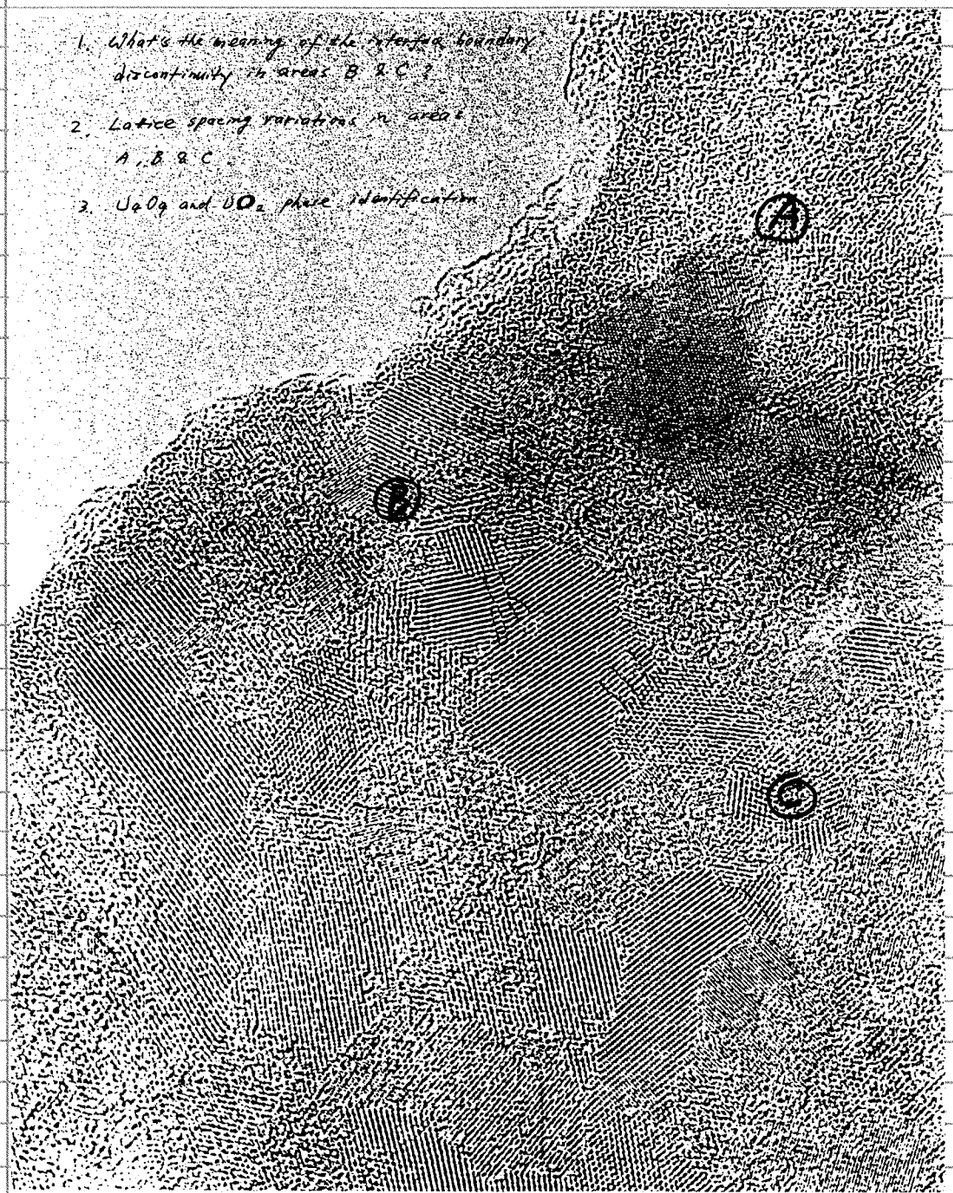

A62319 Area A

Spacing in Dif 1 of Area A: 0.1928 nm
Spacing in Dif 1 of Area A: 0.1635 nm
Spacing in Dif 1 of Area A: 0.1627 nm

Spacing in Dif 2 of Area A: 0.1947 nm
Spacing in Dif 2 of Area A: 0.1606 nm
Spacing in Dif 2 of Area A: 0.1602 nm

Spacing in Dif 3 of Area A: 0.2731 nm
Spacing in Dif 3 of Area A: 0.1605 nm
Spacing in Dif 3 of Area A: 0.1598 nm
Spacing in Dif 3 of Area A: 0.1883 nm

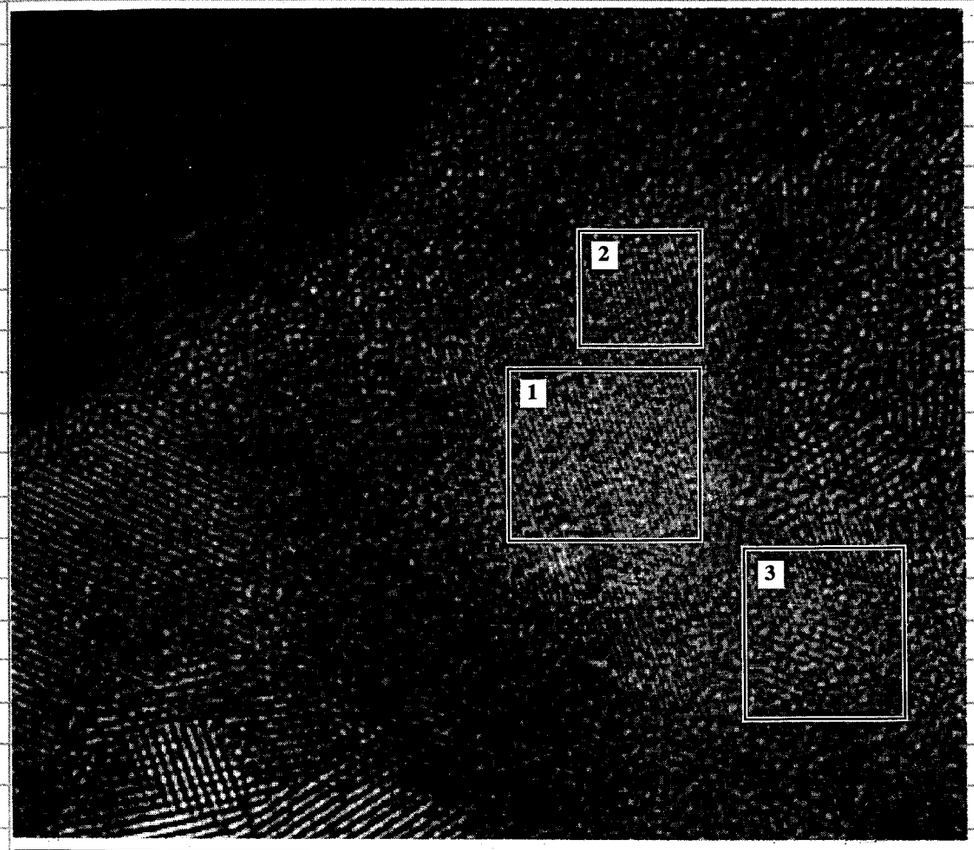

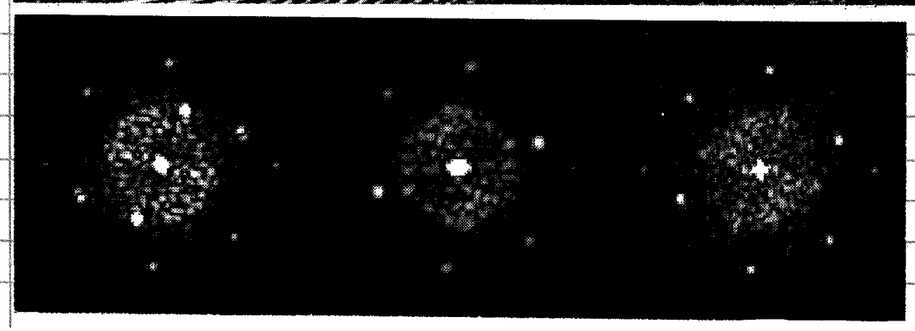

Area B

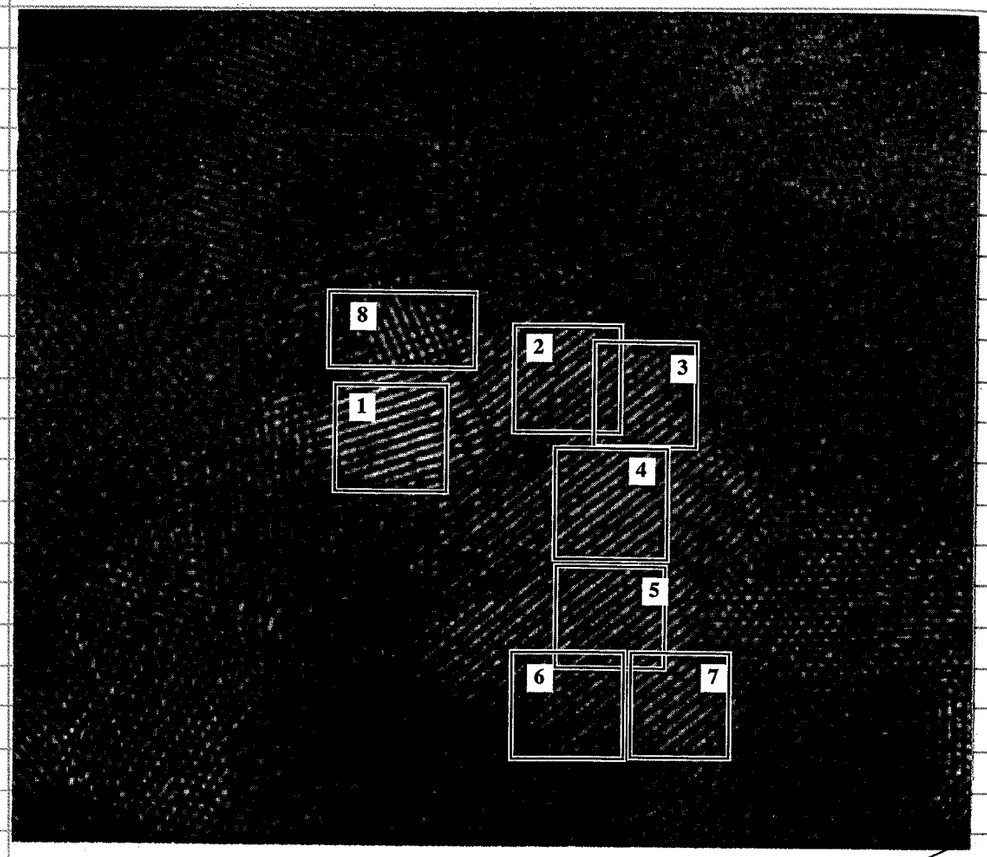

ECP 8/25/94

ECP 8/30/94

area B:

Spacing in Dif 1 of Area B: 0.3079 nm (111)
Spacing in Dif 2 of Area B: 0.3095 nm "
Spacing in Dif 3 of Area B: 0.3090 nm a "
Spacing in Dif 3 of Area B: 0.2870 nm b ?
Angle in Dif 3 of Area B: 55.1°
Spacing in Dif 4 of Area B: 0.3160 nm a (111)
Spacing in Dif 4 of Area B: 0.1448 nm b (321)
Spacing in Dif 5 of Area B: 0.3088 nm a (111)
Spacing in Dif 5 of Area B: 0.1899 nm b (320)
Spacing in Dif 5 of Area B: 0.1463 nm c (321) or (320)
Spacing in Dif 6 of Area B: 0.3090 nm a
Spacing in Dif 6 of Area B: 0.1901 nm b
Spacing in Dif 6 of Area B: 0.1628 nm c
Spacing in Dif 6 of Area B: 0.1441 nm d
Spacing in Dif 7 of Area B: 0.3095 nm a
Spacing in Dif 7 of Area B: 0.1935 nm b
Spacing in Dif 7 of Area B: 0.1438 nm c
Spacing in Dif 8 of Area B: 0.3102 nm a
Spacing in Dif 8 of Area B: 0.3084 nm b

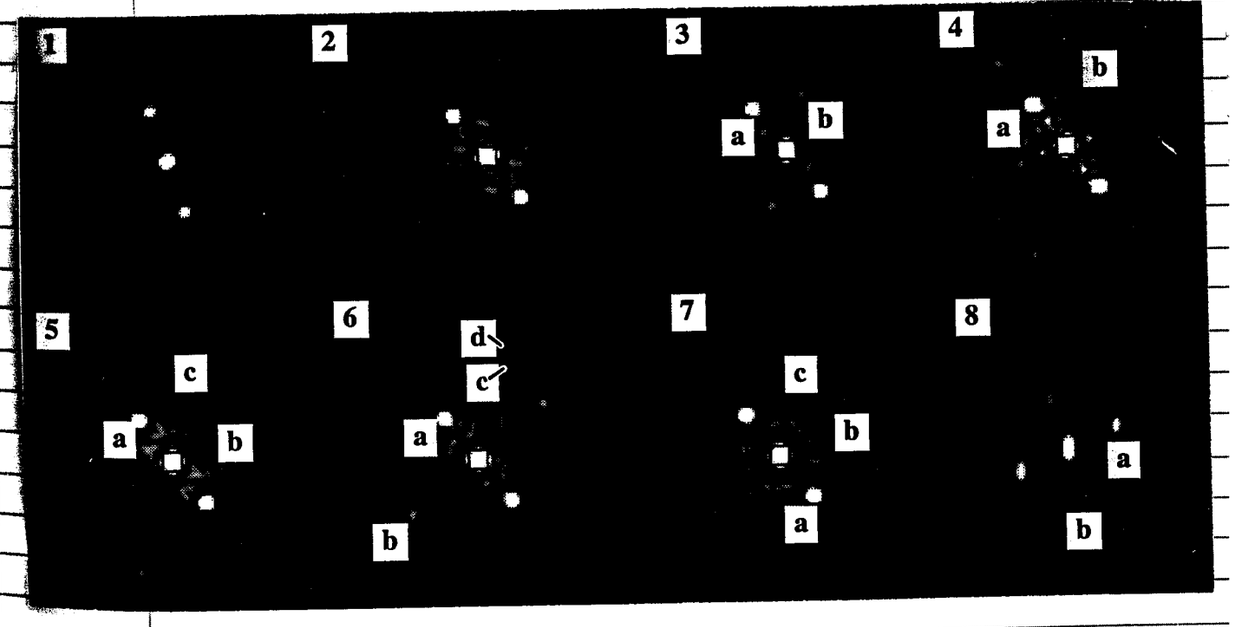

Area C

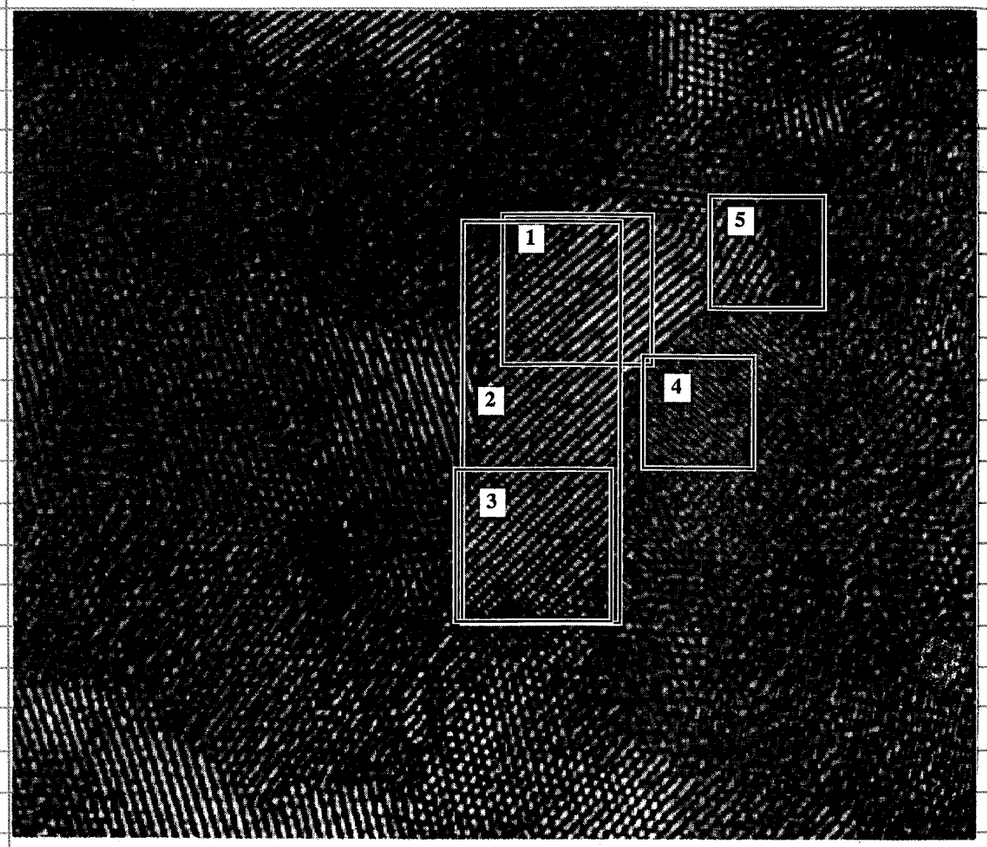

E.C 8/23/94

A62319 area C

Spacing in Dif 1 of Area C: 0.3077 nm
Spacing in Dif 1 of Area C: 0.1907 nm
Spacing in Dif 1 of Area C: 0.8470 nm

Spacing in Dif 2 of Area C: 0.3093 nm
Spacing in Dif 2 of Area C: 0.1891 nm
Spacing in Dif 2 of Area C: 0.1609 nm
Spacing in Dif 2 of Area C: 0.1397 nm

Spacing in Dif 3 of Area C: 0.3101 nm
Spacing in Dif 3 of Area C: 0.1881 nm
Spacing in Dif 3 of Area C: 0.1606 nm
Spacing in Dif 3 of Area C: 0.1397 nm
Spacing in Dif 3 of Area C: 0.4012 nm

Spacing in Dif 4 of Area C: 0.1896 nm
Spacing in Dif 4 of Area C: 0.3415 nm
Spacing in Dif 4 of Area C: 0.1650 nm

Spacing in Dif 5 of Area C: 0.3207 nm
Spacing in Dif 5 of Area C: 0.1892 nm

? Supported Hex

E.C 8/30/94

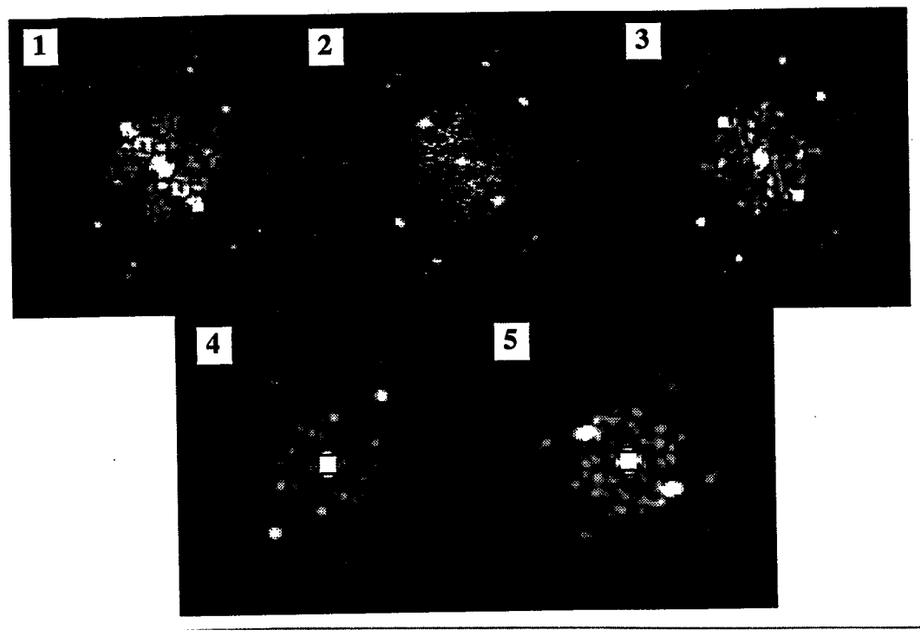

Identification of possible disordered U_4O_9 phase

Sample U2 # A62352

The region of disordered U_4O_9 phase, determined by David Smith of ASU, is denoted with an arrow in the lower magnification print and an area in the digitized image.

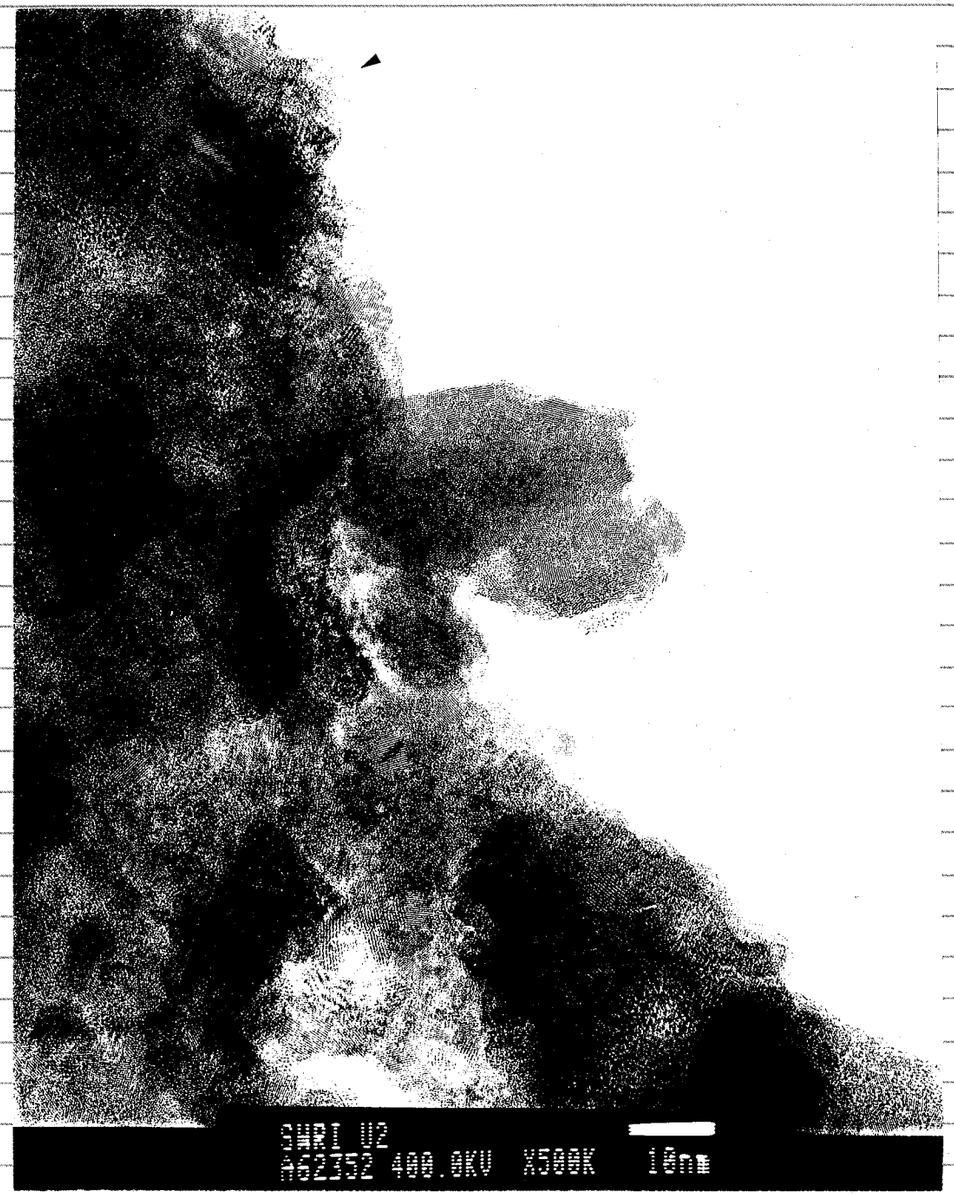

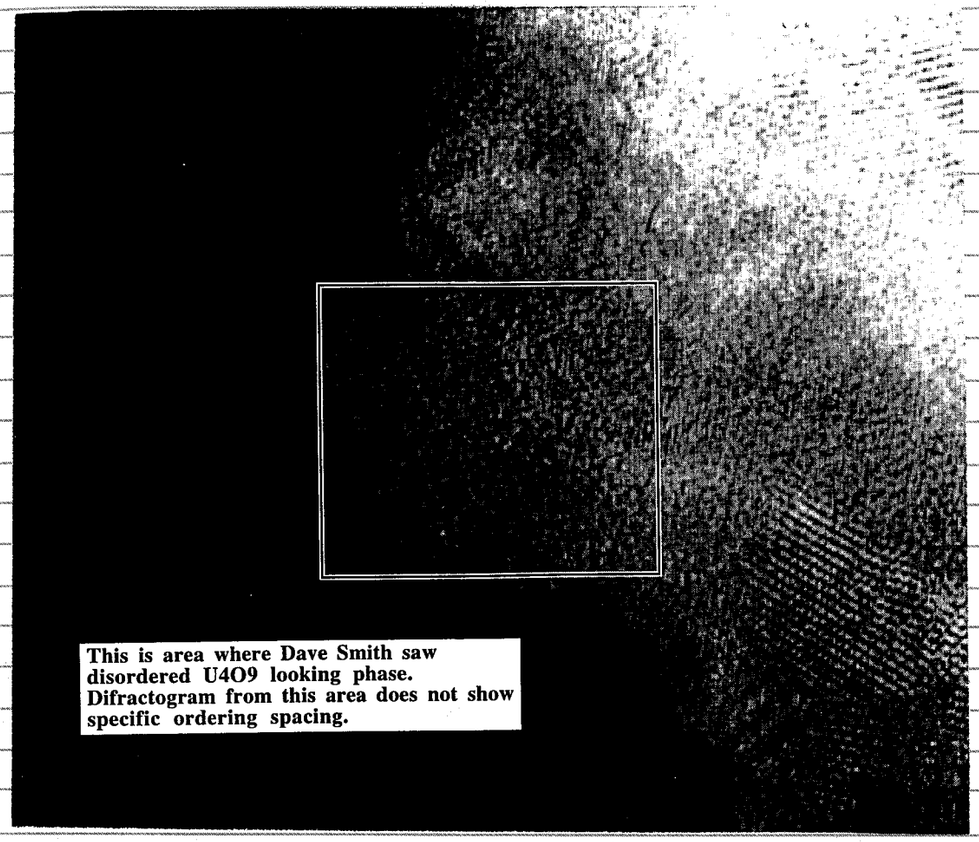

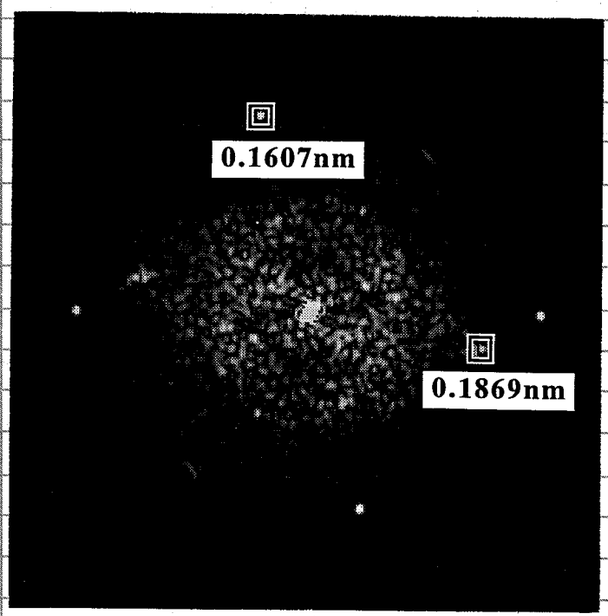

Disc Samples from Colloform Uraninite

7/14/93

TEM Samples from colloform Uraninite

3mm disc samples were punched out from three thin sections containing colloform uraninite, as marked on the following photos.

NOPI-ECP-32 (TS1)

NOPI-ECP-32 (TS3)

ECP 8/25/94

NOP1-ECP-30-TS1

ECP 8/25/94

Colloform Uraninite TEM Samples - Batch 4
(Prepared at UNM)

11/5/93

TEM Thin Foils Preparation at UNM

- Four TEM foils, 30I, 30K, 32K & 32L, were prepared at UNM using ion mill technique with a liquid N_2 cold stage.

NOP1-ECP-32 (TS1)

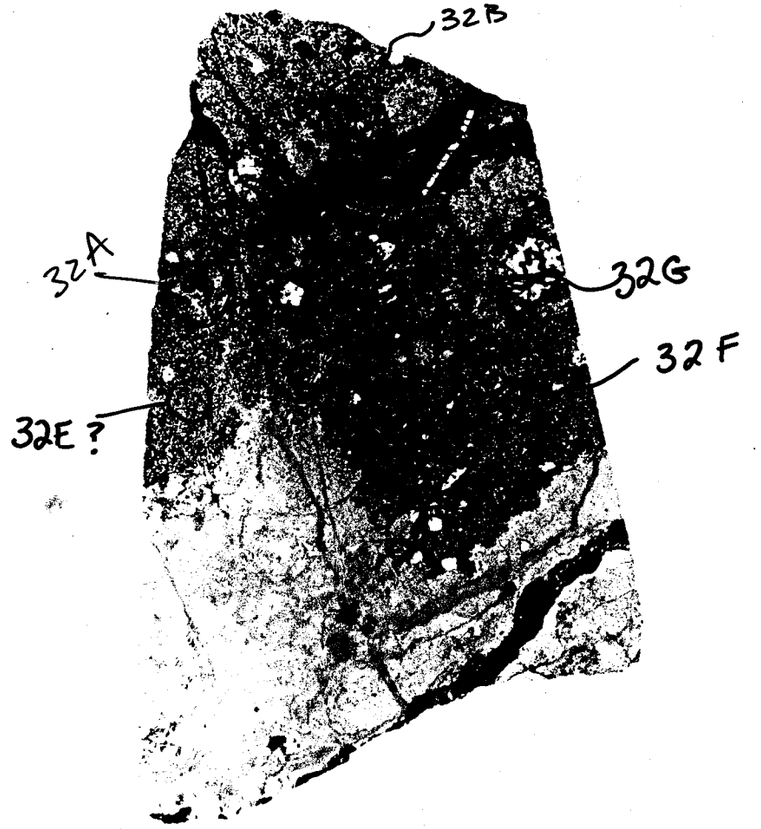

ECP 8/25/94

NOP1-ECP-32(753)

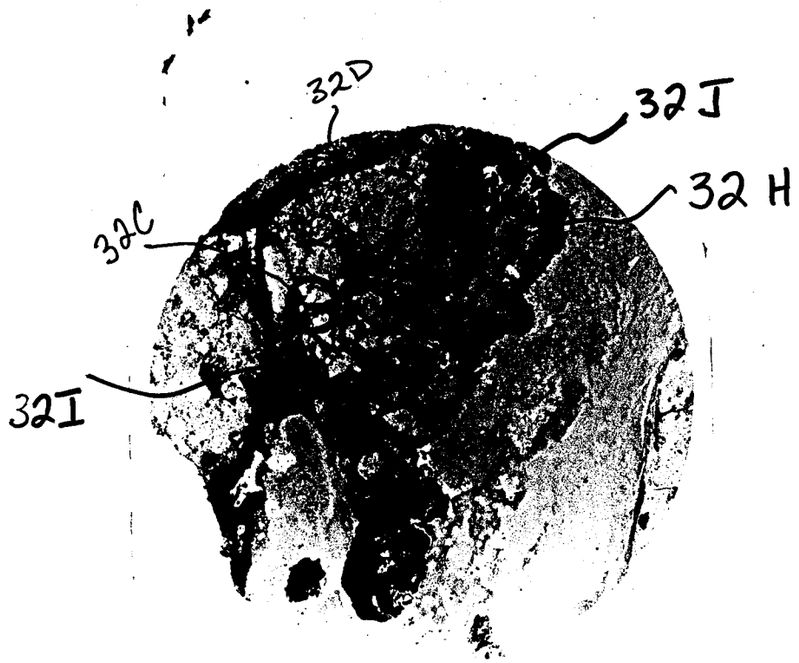

ECP 8/25/84

NOP1-ECP-30-751

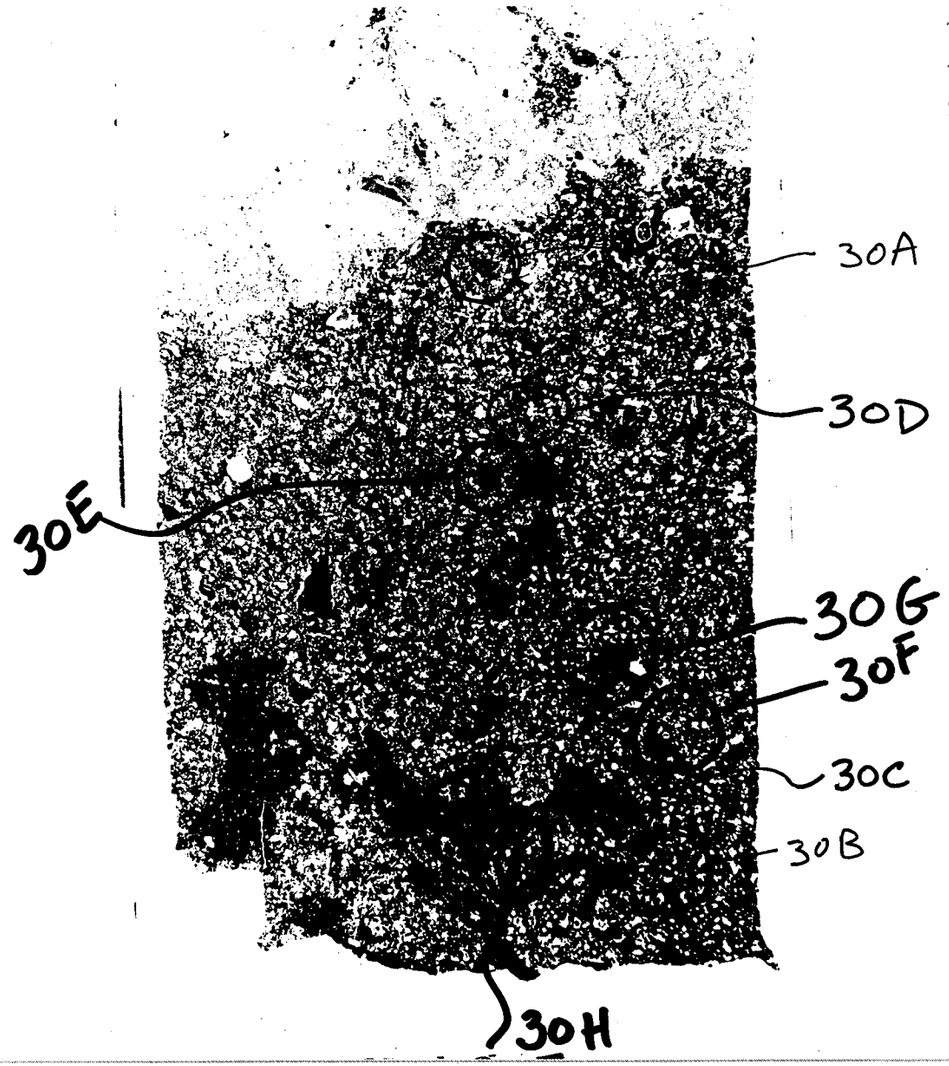

ECP 8/25/84

11/5/93 gp

After ion milling at UNM, Dr. Lu-Min Wang performed some preliminary analyses of the samples.

Below is a letter summary of Dr. Wang's work.

University of New Mexico
Department of Earth & Planetary Sciences
ALBUQUERQUE , NEW MEXICO 87131

TELEPHONE 505/277-7536
FAX 505/277-8843

November 5, 1993

Dr. Yi-Ming Pan
Materials and Mechanics Department
Engineering and Materials Sciences Division
Southwest Research Institute
6220 Culebra Road
P.O. Drawer 28510
San Antonio, Texas 78228-0510

Dear Dr. Pan,

Enclosed please find the preliminary data (32 TEM Bright-field and SAD negatives and 5 EDS spectra) I got with our TEM from the four samples you sent to me earlier. The samples were all ion milled at the liquid nitrogen temperature. There are some thin areas available in each sample for TEM/EDS analysis as shown in the negatives.

The results can be summarized as follows (incomplete):
(1) In sample 30I, two kinds of "rods" were found in a matrix which only contains Si. One kind of rod contains both Al and Si, the other contains mainly U which appears much darker (lighter in the negative). Please remember our EDS system on the 2000FX can not detect elements lighter than Na, so these rods could be UO_2..
(2) In sample 30K, matrix contains also only Si and it was determined to be single crystalline (see the SAD pattern 2876). Dark UO_2 rods and blocks were found in the matrix (see negatives for their distribution). Also, some bright Al and Si containing regions (single crystalline) and a dark crystal which only has Fe and S were found.
(3) In sample 32K, some big U-rich areas with a lot of gas bubbles was observed (2881, 2882). A region with granular grains contains only Fe. U-rich phases are polycrystalline with very small grain sizes (neg. 2878-2880, ~~2883~~).
(4) Sample 32U has large U rods and blocks. The brighter region (darker on the negative) contains both Al and Si. At least one large U rod seemed to be single crystalline (neg. 2891).

I have spent 4 hours on the microscope for your samples. So we will bill you totally for $640 ($400 for sample preparation and $240 for TEM analysis).

As I told you on the phone, our new JEM2010 microscope is in the process of installation. The new microscope will have an ultra-thin window EDS system, with that we are going to be able to detect oxygen and carbon. Also, the new microscope's point resolution is 1.9 Å, much better than that of our current 2000FX (3.0Å).

I am looking forward to more collaboration with you in the future.

Sincerely yours,

Lu-Min Wang, Ph.D.
Senior Research Scientist

Data is kept in 3-ring binder entitled "TEM Work at UNM" and consists of EDS spectra and photographs.

Pages 1 through 65 of this Scientific Notebook were reviewed for compliance with QAP-001 in response to Corrective Action Request 94-02. Corrections and clarifications were made as appropriate. In some cases, the date of a change will reflect the date of this review rather than the date of the original Scientific Notebook entry.

Randy Folck QA
SwRI
10/14/94

12/5/94

Uranium Fixation in Fracture-Filling Materials
- Initial Entry

Objective:

- Determine the role of secondary mineral formation on uranium fixation in fracture-filling materials at the Nopal deposit.

Approach:

Selected fracture-filling materials will be analyzed using transmission electron microscopy (TEM) with an energy dispersive x-ray spectroscopy (EDS) attachment to determine the uranium fixation mechanism.

Specimen Description:

Two fracture-filling materials, NOPI-418-TS1 and NOPI-420-TS1, were selected, which correspond to the sampling locations of 11.7 and 6.2, respectively, along the E-W fracture. These materials were left over from petrographic thin section preparation and impregnated with epoxy. The fracture-filling material consists of jarosite [$KFe_3(SO_4)_2(OH)_6$], goethite [α-FeO·OH], hematite [Fe_2O_3], Kaolinite [$Al_2Si_2O_5(OH)_4$], and quartz [SiO_2].

Yifeng Pan
12/5/94

12/12/94 TEM Thin Foils Preparation From 418 & 420 Materials 1/5/95

- Thin section slices from both 418 & 420 materials were sectioned using Isomet with an initial thickness setting of 0.8 mm. The thickness of the slices were measured to be ground 250 μm
- Disks of 3 mm in diameter were punched out from the areas of interest and mechanically thinned to approximately 10-20 μm using a dimpler.
- The disks were then placed on a supporting copper grid and further thinned to perforation using an ion-beam milling machine. The ion-milling conditions were:

  Gun voltage 3.5 KV
  Gun current 1 mA (2 guns / 0.5 mA each)
  Tilt angle 10-20 degree
  Liquid nitrogen cold-stage sample holder

Yi Pan
1/4/95

Preliminary Microstructure Examination and Chemical Analysis of Specimens 418-3 & 420-2

Preliminary microstructure and chemical analysis was performed for both NOPI-418-TS1 and NOPI-420-TS1 specimens.

1) SEM photos for thin-foil specimen 418-3

photo # 1 (418-3)

Photo #2 (418-3)

2) SEM Photos for specimen 420-2

Photo #1 (420-2)

Photo #2 (420-2)

3) Composition counts for specimen 420-3 by STEM/EDS

	Si	S	Cr	Fe	Cu	Mo	U	K
Sample 420-3 Single-Side Ion-Milled								
Hole Analysis I	0	0	0	2	14	0	0	0
Dark Inclusion 1 I	28	(14)	0	31	246	0	0	21
Dark Inclusion 2 I	82	40	57	84	745	0	0	56
Matrix I	67	0	0	63	454	0	0	51
Copper Grid 1 I	57	31	0	112	2435	0	0	0
Copper Grid 2 I	110	0	0	131	3560	0	0	0

4) Composition counts for specimen 418-3 by STEM/EDS

	Si	S	Cr	Fe	Cu	Mo	U (Ld)
Sample 418-3 Double-Side Ion-Milled							
Hole Analysis I	0	0	0	12	2	0	0
Dark Inclusion 1 I	45	95	34	131	606	26	6
Dark Inclusion 2 I	13	32	19	38	183	13	(2)*
Light Inclusion 1 I	8	26	5	26	60	8	(1)
Light Inclusion 2 I	10	17	5	21	42	5	(2)
Matrix 1 I	21	61	8	50	67	22	(3)
Matrix 2 I	9	23	4	19	24	7	0
Single-Side Ion-Milled (After Perforation)							
Hole Analysis I	0	0	0	12	2	0	0
Dark Inclusion 1 I	48	74	22	256	126	17	(4)
Dark Inclusion 2 I	29	20	19	181	163	(4)	0
Dark Inclusion 3 I	26	26	24	150	184	(4)	0
Matrix 1 I	14	(7)	0	34	9	0	0
Matrix 2 I	12	13	0	43	13	0	0
Matrix 3 I	7	22	0	31	9	5	0

*( ): Background / Noise Signal

JP 1/7/95

1/9/95

Chemical Analysis and Phase Identification of Foil 420-2

Chemical analysis was conducted on various locations of Foil 420-2 in an attempt to identify possible phases.

1) Composition counts were summarized as follows.

	Al	Si	S	K	Fe	Cu	Mo
Sample 420-2 Double-Side Ion-Milled							
Photo No 8688 Dark Inclusion I		7	6	5	4	39	
Granular Matrix I		10	6	3	4	24	
Transl Area I	6	18		4			
Photo No 8690 Dark Inclusion I		7	16		8	38	5
Granular Matrix I		5	14		7	30	4
Photo No 8692 Laminar Structure I		3			12		
Transl Area I		5	8		3		
Photo No 8694 Laminar Structure I		4			43		
Top Dark Area I					19		
Transl Area I	4	8					

Photo No 8696							
Dark Band							
I		6			26		
Light Band							
I	9	12					
Photo No 8699							
Laminar Structure							
I					11		
Granular Structure							
I	2	6	9	2	4	17	1
Photo No 8702							
Laminar Structure							
I		4			43		
Top Dark Area							
I		4			33		
Top Light Area							
I					7		
Granular Strucutre							
I		3	3		4	19	
Transl Area							
I		7	5				

J. J. Po
1/19/95

2) High emission chemical analysis was performed in order to distinguish uranium peaks.

	Al	Si	S	K	Fe	Cu	Mo	U (Ld1)
Sample 420-2								
High emission measurements								
Photo No 8692								
Spot size 6(25nm)/30sec								
Laminar 1								
I		12		6	100	9		
Laminar 2								
I		15	6	9	120	9		
Laminar 3								
I		3	4	7	33	4		
Transluent								
I	12	43		4	4	5		
Granular								
I	10	7	23	4	15	57	8	
Spot size 5(50nm)/1min								
Laminar 1								
I	(17)	47	20	36	564	35	(4)	(5)*
Laminar 1(2min)								
I	(34)	116	37	83	1265	92	9	(6)
Laminar 1(3min)								
I	56	181	58	123	1916	132	11	(8)
Laminar 2								
I	24	62	24	41	672	41	8	(4)
Laminar 22								
I	25	50	23	37	587	45	3	(3)
Granular								
I	16	21	113	10	42	240	25	(3)

* ( ): Background / Noise Signal

3) Chemical analysis of laminar structure for uranium variation along or perpendicular to laminar.

	Al	Si	S	K	Fe	Cu	Mo	U (Mα)	U (Mβ)
Sample 420-2									
High emission measurements									
Photo No 8692									
Spot size 6(25nm)/60sec									
Along laminar									
Position 1									
I	(3)*	8	5	11	69	5		9	11
Position 2									
I	(7)	14	8	17	105	12		14	13
Position 3									
I	(6)	13	6	11	82	7		8	11
Position 4									
I	(7)	9	13	27	98	13		15	21
Position 5									
I	(7)	9	7	18	100	8		11	18
Perpendicular to laminar									
Position 1									
I	(2)	6	4	10	50	6		6	10
Position 2									
I	(6)	14	9	16	79	10		15	16
Position 3									
I	(9)	12	10	20	128	15		17	20
Position 4									
I	11	19	14	19	126	12		16	19
Position 5									
I	13	15	17	33	124	17		28	33
Outside laminar									
Transluent									
I	21	55	8	7	2	7		(6)	(4)
Granular									
I	9	12	29	9	8	31	11	(9)	(6)

*( ) : Background / Noise Signal

4) Electron diffraction analysis of Goethite phase from computer simulation.

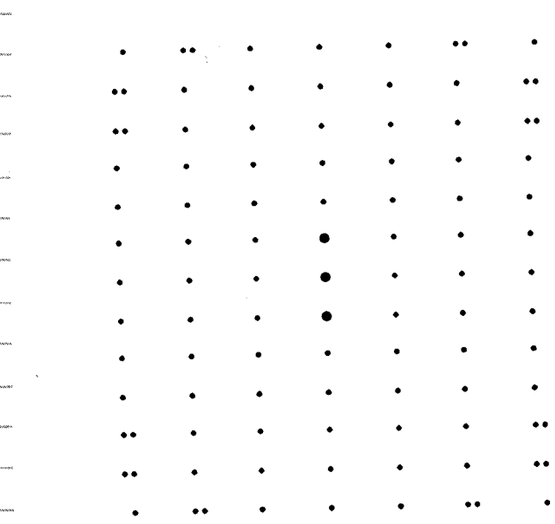

Zone axis
[01$\bar{2}$]

M D Pa
1/26/95

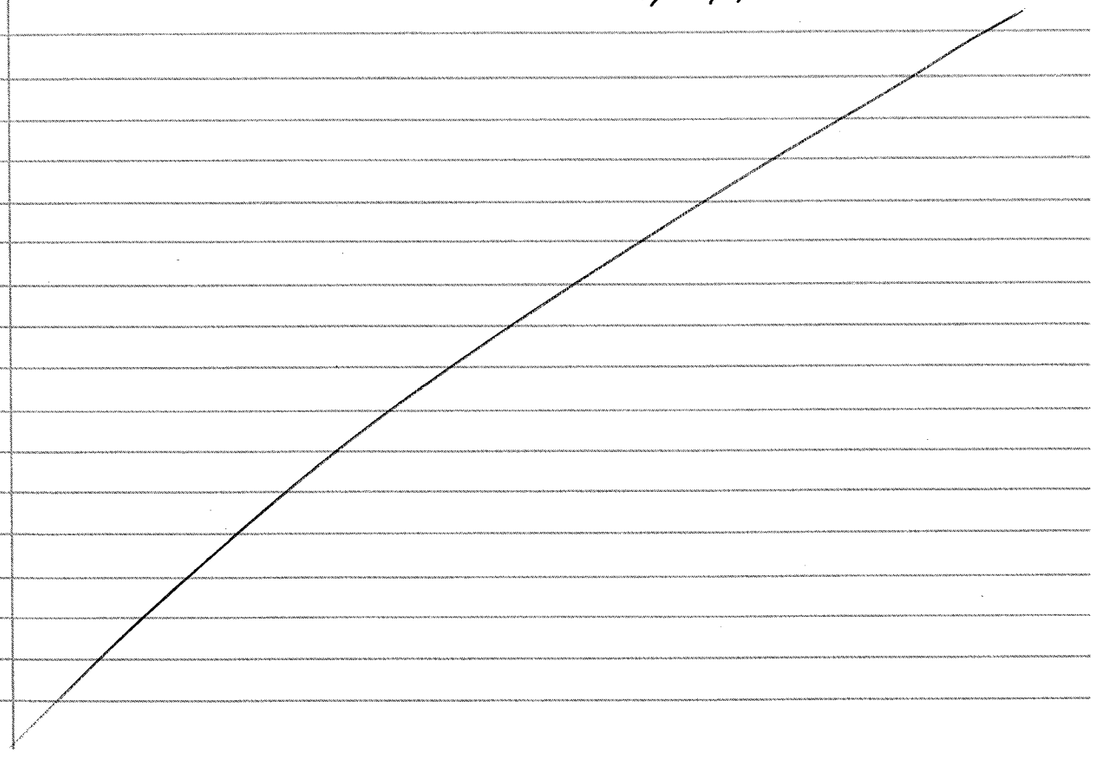

1/29/95

STEM Microstructure and Diffraction of Foil 420-2

1) STEM microstructure photos from foil 420-2

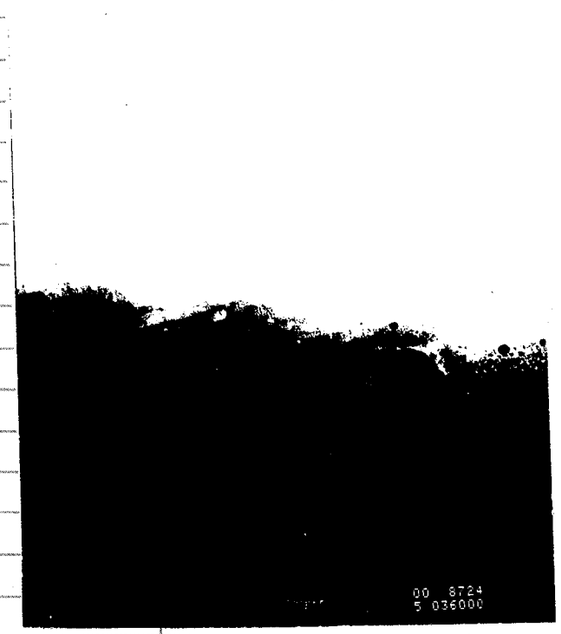

#8724

#8725
Enlarged area in #8724

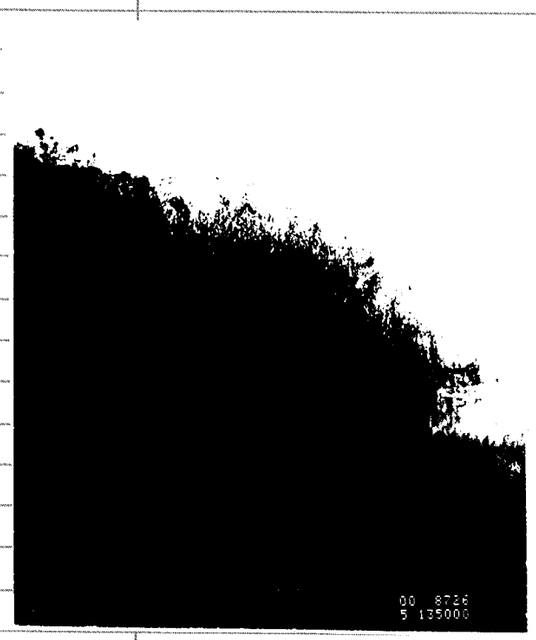

#8726
Enlarged area in #8724

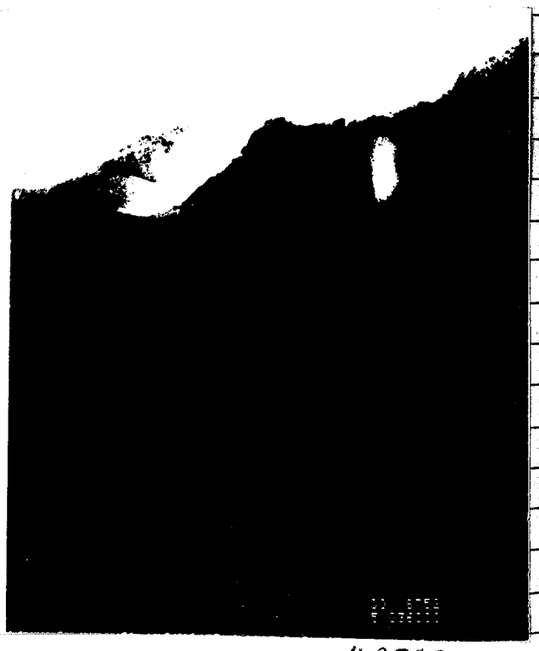

#8752

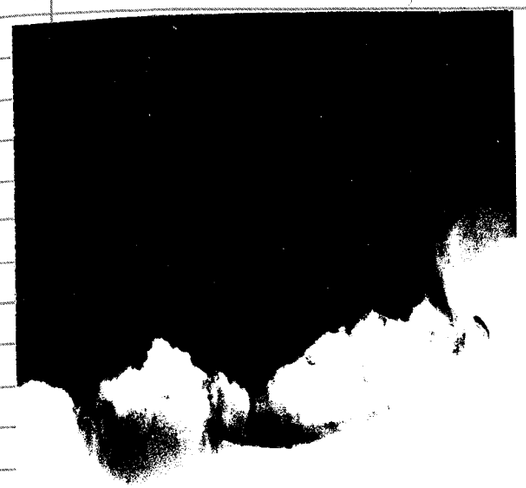

#8728

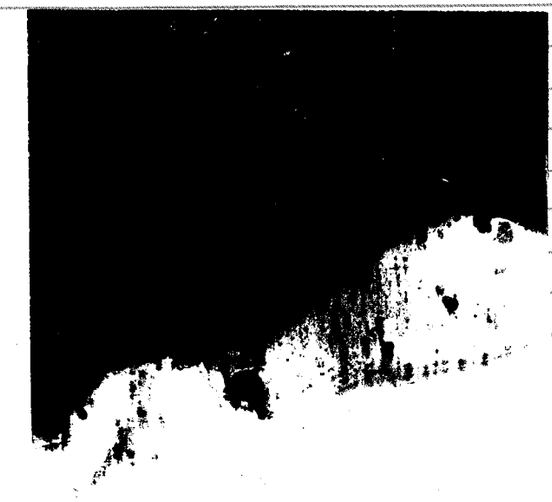

#8730

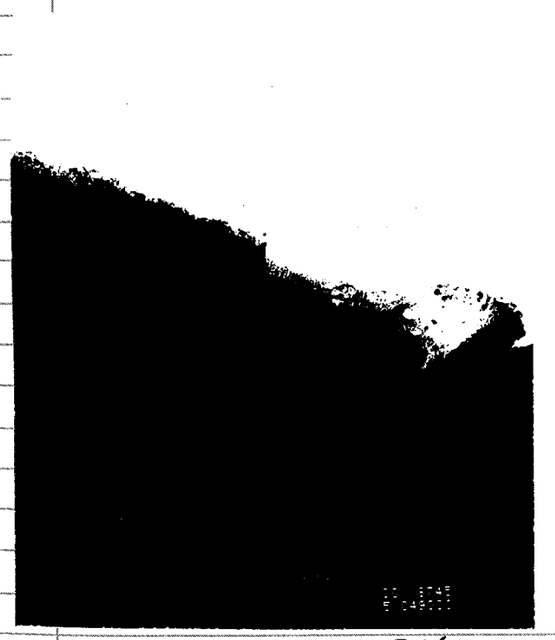

#8745

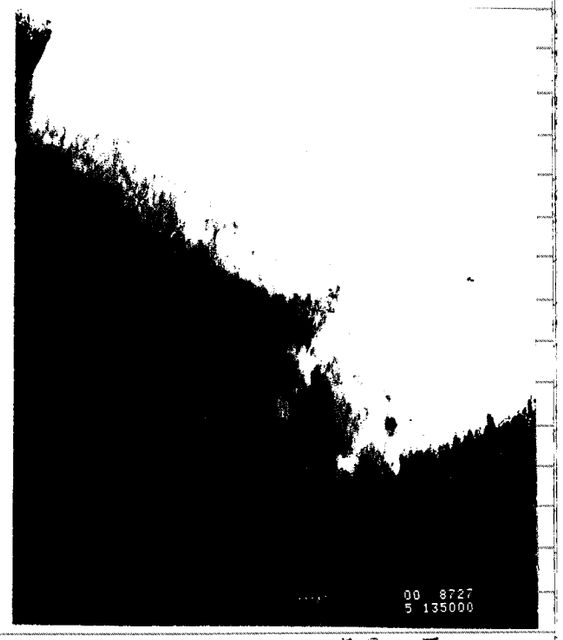

#8727
Enlarged area in #8745

2) Electron diffraction patterns from Hematite phase

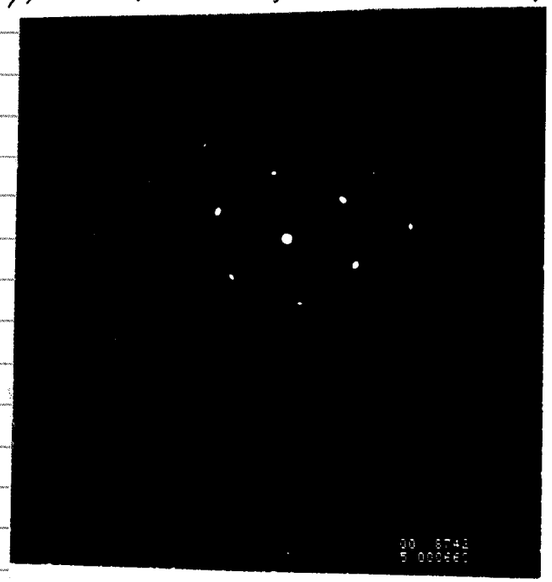

SADP $\lambda L = 2.70$ cm·Å

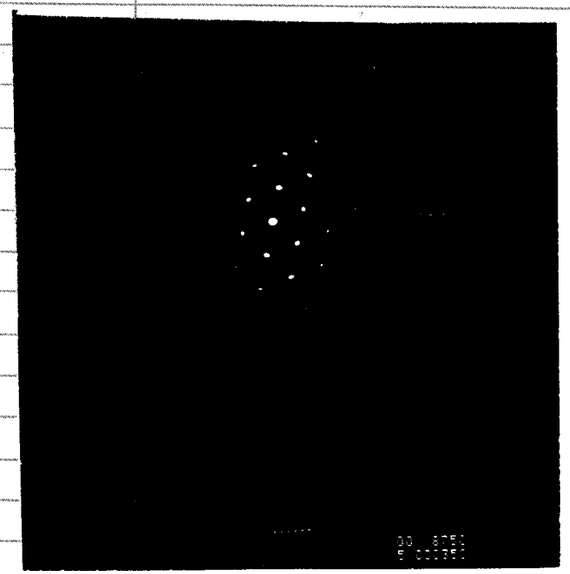

SADP $\lambda L = 1.32$ cm·Å

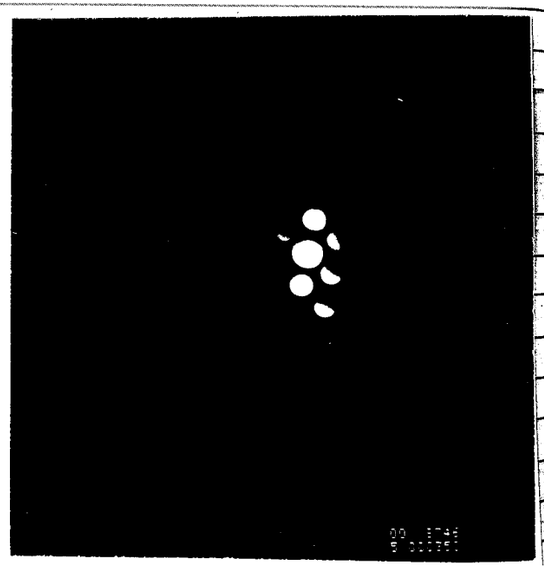

Microdiffraction (Spot size 6) $\lambda L = 1.32$ cm·Å

2/1/95

2/6/95 Chemical Analysis of Foil 418-3

Composition counts from various locations of Foil 418-3 were summarized as follows.

	Al	Si	S	Cr	Fe	Cu	U
Sample 418-32 Double-Side Ion-Milled Spot size 5(50nm)/30sec							
Photo No 8759 Loc A1 I	12	19	30	8	110	71	5
Loc A2 I	8	23	21	11	92	62	5
Photo No 8762 Loc B1 I		22			200	11	
Loc B2 I		43			325	20	
Photo No 8764 Loc C1 I		23	15		188	15	
Loc C2 I	10	16	32	11	45	90	
Photo No 8768 Loc D1 I	5	17	7		102	4	
Loc D2 I	11	24			233	9	
Photo No 8774 Loc E1 I		19			385	153	
Loc E2 I		18			413	175	

2/8/95

2/9/98 Nanoprobe Analysis of Laminar Structure in Foil 420-2

Chemical analysis of laminar structure in Foil 420-2 was conducted using different probe techniques. both microprobe and nanoprobe. The spot size was 25 μm for microprobe and only 2 nm for nanoprobe. Composition counts were presented below.

	Al	Si	K	Fe	Cu	Ca
Sample 420-24						
High emission measurements						
Photo No 8724						
Spot size 6(25nm)/30sec						
Holy area-1						
I	11	20		18	4	
Holy area-2						
I	18	25		16	4	
Dark area-1						
I		5		46	5	
Dark area-2						
I				27	4	
Light area						
I				16		
Photo No 8728/8730						
Light area-1						
I		5		19	14	
Light area-2						
I		7	4	16	11	6
Light area-3						
I	4	5		12	4	

	Al	Si	S	K	Fe	Cu	Mo	U
Sample 420-25								
Nanoprobe analysis(TEM/EDS)								
Spot size 6(2nm)								
Photo No 8692(Laminar structure)								
Position 1(30sec)								
I		7	7	4	9	9	2	
Position 2(60sec)								
I	5	9	11	7	34	19	4	6

Note: Specific spot of analysis can't be located when focusing electron beam.

2/10/98

2/27/95 Summary and Recommendation

MEMORANDUM

February 27, 1995

To: James D. Prikryl

From: Yi-Ming Pan/Computation Research Professionals, Inc. Yi-Ming Pan

Subject: CNWRA Project No. 20-5704-063
"Uranium Fixation in Fracture-Filling Materials"
Summary and Recommendation

The object of this investigation is to analyze the role of secondary mineral formation on uranium fixation in fracture-filling materials at the Nopal deposit using transmission electron microscopy (TEM). The major findings of this investigation may be summarized as follows:

1. The use of energy-dispersive x-ray spectroscopy (EDS) and electron diffraction techniques in the analytical electron microscope has characterized the major secondary minerals such as goethite, hematite and amorphous Fe-oxide in the fracture-filling materials at the Nopal deposit. These minerals shows distinct features in terms of phase morphology, chemical composition and diffraction pattern.

2. Uranium concentrations have been measured to be sited on the goethite phase which shows a laminar structure with a lath thickness of approximately 5~~μm~~ nm. It was observed that the uranium concentrations along and normal to the laminas varied according to the total EDS counts using a focused electron probe of about 25nm diameter. The variation of the uranium concentrations measured normal to the laminas is greater than that seen along the laminas.

3. No discrete uranium-containing phase has been observed in this investigation. Nonetheless, the inhomogeous uranium distribution within goethite mentioned above may be associated with other fine uranium bearing phases that may not be discernible under a conventional TEM. Detailed characterization requires the application of high resolution electron microscopy (HREM) techniques.

4. Previous analysis of natural uraninite alternation by high resolution electron microscopy has suggested that HREM will be an effective tool in determining the mechanism of uranium fixation in fracture-filling materials at atomic levels.

Yi-Ming Pan 2/27/95

cc: Dr. English C. Pearcy

this project was ended so that the U.S. goverment could more closely balance its budget.

Do not go gentle into that dark night...

E.C. Pearcy

12/19/96